11-8-2022

Cardiac myosin-specific autoimmune T cells contribute to immune-checkpoint-inhibitor-associated myocarditis

Taejoon Won

Hannah M. Kalinoski

Megan K. Wood

David M. Hughes

Camille M. Jaime

See next page for additional authors

Authors

Taejoon Won, Hannah M. Kalinoski, Megan K. Wood, David M. Hughes, Camille M. Jaime, Paul Delgado, Monica V. Talor, Ninaad Lasrado, Jay Reddy, and Daniela Čiháková

Cell Reports

Article

Cardiac myosin-specific autoimmune T cells contribute to immune-checkpoint-inhibitor-associated myocarditis

Graphical abstract

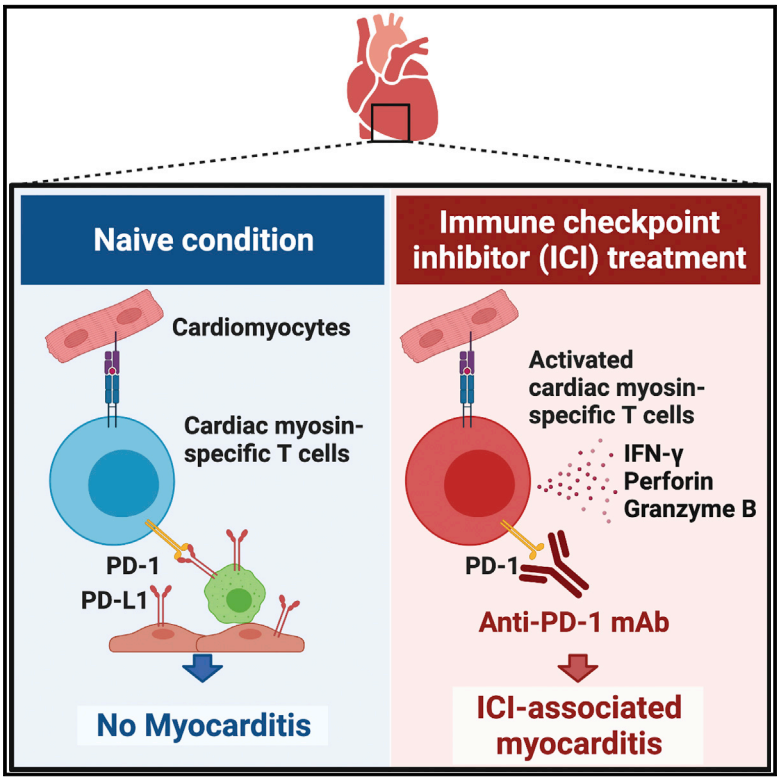

Highlights

- PD-1 inhibitor treatment alone causes myocarditis development in A/J mice
- Cardiac-myosin-specific T cells drive PD-1 inhibitor-induced myocarditis in mice
- Cardiac-myosin-specific autoimmune T cells are present in naive mouse hearts
- Cardiac-myosin-specific autoimmune T cells express PD-1 during naive conditions

Authors

Taejoon Won, Hannah M. Kalinoski, Megan K. Wood, ..., Ninaad Lasrado, Jay Reddy, Daniela Čiháková

Correspondence

cihakova@jhmi.edu

In brief

Won et al. demonstrate that PD-1 inhibitor treatment alone induces myocarditis in A/J mice, creating a mouse model for immune-checkpoint-inhibitor-associated myocarditis. Cardiac myosin-specific autoreactive T cells drive the pathogenesis of PD-1 inhibitor-induced myocarditis in mice. PD-1-expressing cardiac myosin-specific T cells are present in the heart during naive conditions.

Won et al., 2022, Cell Reports *41*, 111611
November 8, 2022
https://doi.org/10.1016/j.celrep.2022.111611

CellPress

Cell Reports

CellPress
OPEN ACCESS

Article

Cardiac myosin-specific autoimmune T cells contribute to immune-checkpoint-inhibitor-associated myocarditis

Taejoon Won,[1] Hannah M. Kalinoski,[2] Megan K. Wood,[2] David M. Hughes,[3] Camille M. Jaime,[4] Paul Delgado,[2] Monica V. Talor,[1] Ninaad Lasrado,[5,6] Jay Reddy,[5] and Daniela Čiháková[1,2,7,*]

[1]Department of Pathology, Johns Hopkins University School of Medicine, Baltimore, MD 21205, USA
[2]W. Harry Feinstone Department of Molecular Microbiology and Immunology, Johns Hopkins University Bloomberg School of Public Health, Baltimore, MD 21205, USA
[3]Department of Chemical and Biomolecular Engineering, Johns Hopkins University Whiting School of Engineering, Baltimore, MD 21218, USA
[4]Graduate Program in Immunology, Johns Hopkins University School of Medicine, Baltimore, MD 21205, USA
[5]School of Veterinary Medicine and Biomedical Sciences, University of Nebraska-Lincoln, Lincoln, NE 68583, USA
[6]Center for Virology and Vaccine Research, Beth Israel Deaconess Medical Center, Harvard Medical School, Boston, MA 02215, USA
[7]Lead contact
*Correspondence: cihakova@jhmi.edu
https://doi.org/10.1016/j.celrep.2022.111611

SUMMARY

Immune checkpoint inhibitors (ICIs) are an effective therapy for various cancers; however, they can induce immune-related adverse events (irAEs) as a side effect. Myocarditis is an uncommon, but fatal, irAE caused after ICI treatments. Currently, the mechanism of ICI-associated myocarditis is unclear. Here, we show the development of myocarditis in A/J mice induced by anti-PD-1 monoclonal antibody (mAb) administration alone without tumor cell inoculation, immunization, or viral infection. Mice with myocarditis have increased cardiac infiltration, elevated cardiac troponin levels, and arrhythmia. Anti-PD-1 mAb treatment also causes irAEs in other organs. Autoimmune T cells recognizing cardiac myosin are activated and increased in mice with myocarditis. Notably, cardiac myosin-specific T cells are present in naive mice, showing a phenotype of antigen-experienced T cells. Collectively, we establish a clinically relevant mouse model for ICI-associated myocarditis and find a contribution of cardiac myosin-specific T cells to ICI-associated myocarditis development and pathogenesis.

INTRODUCTION

In the last decade, immune checkpoint inhibitors (ICIs) targeting PD-1 and CTLA-4 have become a groundbreaking therapy to effectively treat various types of cancers such as melanoma, non-small cell lung cancer, head and neck squamous cell carcinoma, colorectal cancer, and urothelial carcinoma.[1,2] However, over 70% of patients with cancer treated with ICIs experienced immune-related adverse events (irAEs) in the heart, lung, liver, intestine, and skin, ranging from mild to severe grades.[3–5] Myocarditis occurring in ICI-treated patients with cancer is an uncommon irAE but is fatal, with a 40% reported mortality rate.[6] Patients with ICI-associated myocarditis present chest pain, cardiac troponin level elevation, and abnormality on electrocardiogram (ECG), echocardiogram, or cardiac magnetic resonance imaging, and the clinical presentations may vary between cases.[7–11] Histologically, infiltrating cells in ICI-associated myocarditis were composed of mostly T cells and macrophages, showing the predominance of $CD8^+$ T cells over $CD4^+$ T cells.[10–14] Since PD-1 and CTLA-4 are expressed mainly in T cells, researchers speculated that T cells play a crucial role in the development of ICI-associated myocarditis.[15] However, it is unclear whether ICI-associated myocarditis is caused by autoimmune T cells recognizing cardiac antigens or off-target effects of anti-tumor T cells by cross-reactivity.

Previous animal studies have shown cardiotoxicity of inhibition of the PD-1/PD-L1 pathway, but there were no appropriate mouse models that completely mimic the human ICI-associated myocarditis. PD-1 blockade by neutralizing antibody worsened the severity of myocarditis induced by cardiac myosin peptide immunization or CVB3 infection.[16,17] PD-1-deficient mice have been used for studying ICI-associated myocarditis; however, to induce spontaneous development of myocarditis, PD-1-deficient (*Pdcd1*$^{-/-}$) C57BL/6 mice necessitated additional conditions such as crossing to autoimmune-prone MRL mice, introducing a haploinsufficient *Ctla4* gene, or using genetically engineered T cells.[18–21] *Pdcd1*$^{-/-}$ mice on BALB/c background spontaneously developed myocarditis and dilated cardiomyopathy mediated by an anti-cardiac troponin I (cTnI) autoantibody, which is a distinct mechanism from ICI-associated myocarditis.[22,23] To better understand the etiology and pathogenesis of ICI-associated

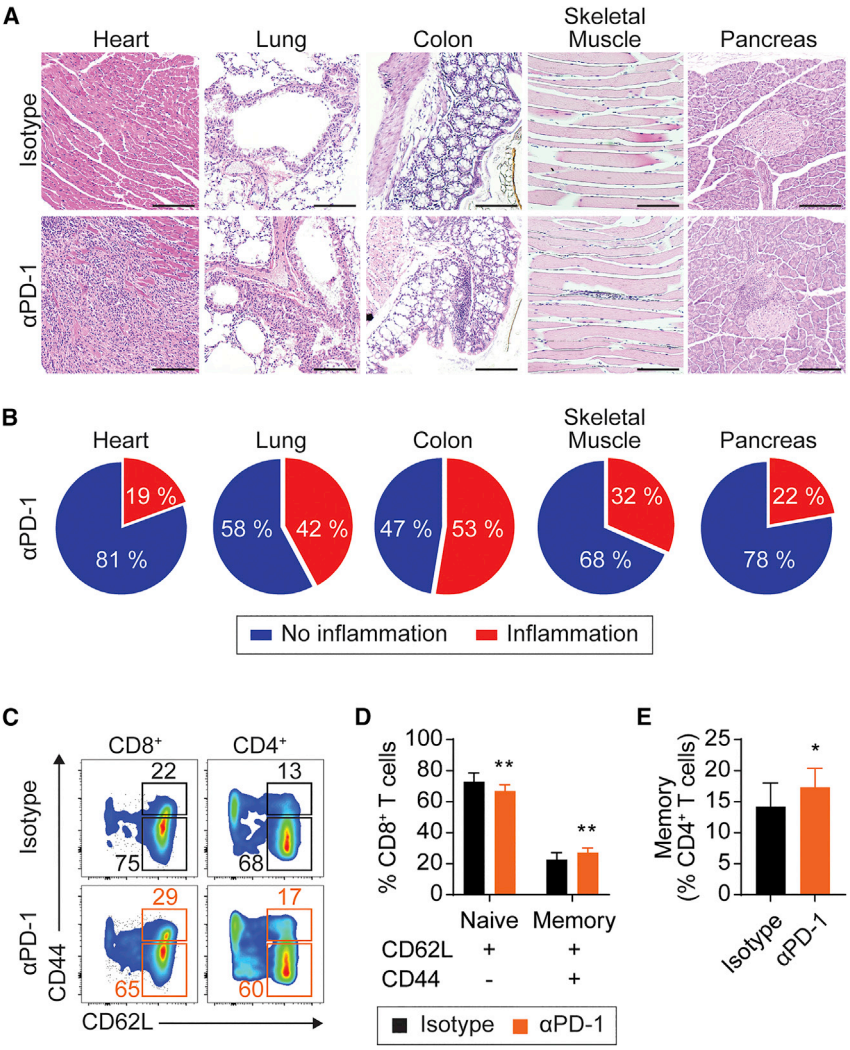

Figure 1. αPD-1 mAb treatment induces irAEs in multiple organs in mice

(A) Representative images of H&E staining on hearts, lungs, colons, skeletal muscles, and pancreases from αPD-1 mAb-treated A/J mice and isotype controls. Scale bars: 100 μm.

(B) Pie charts showing the incidence of inflammation in hearts, lungs, colons, skeletal muscles, and pancreases after αPD-1 mAb treatment.

(C) Flow cytometry analysis of CD62L and CD44 expression in peripheral blood mononuclear cell (PBMC) $CD8^+$ and $CD4^+$ T cells from αPD-1 mAb-treated mice and isotype controls.

(D and E) Cell frequency of naive ($CD62L^+CD44^-$) and memory ($CD62L^+CD44^+$) subsets in PBMC $CD8^+$ T cells (D) and memory subset in PBMC $CD4^+$ T cells (E) from mice with αPD-1 mAb or isotype Ab treatment.

Pooled data of two experiments are shown. Student's t test was used for statistical analysis. *$p < 0.05$; **$p < 0.005$.

myocarditis, a proper mouse model established on the immunocompetent strain is needed.

Cardiac myosin is a heart antigen recognized by autoantibodies in patients with myocarditis and dilated cardiomyopathy.[24–27] Cardiac myosin peptides have the capacity to stimulate T cells isolated from patients with myocarditis.[28] Animal studies support the involvement of cardiac myosin as a potent heart-specific autoantigen stimulating T cells during myocarditis. Immunization with cardiac myosin or its shortened peptide caused experimental autoimmune myocarditis (EAM) development in mice, exhibiting elevated anti-myosin autoantibody levels and increased myosin-specific T cells.[29–31]

In this study, we induced ICI-associated myocarditis in A/J mice, an immunocompetent strain, only by injecting PD-1 neutralizing monoclonal antibody (mAb). Autoimmune inflammation was also found in other organs such as the lung, colon, skeletal muscle, and pancreas of PD-1 inhibitor-treated mice. We suggest cardiac myosin as a potential target of pathogenic T cells in ICI-associated myocarditis. Mice with PD-1 inhibitor-induced myocarditis showed an increased number of cardiac-myosin-specific T cells in the heart. We also found the presence of PD-1-expressing myosin-specific T cells in naive mice, suggesting activation of heart antigen-reactive T cells by PD-1 inhibitor as a possible mechanism of ICI-associated myocarditis.

RESULTS

αPD-1 mAb treatment induces multiorgan irAEs in mice

To establish whether PD-1 blockade can cause irAEs in immunocompetent mice, we injected αPD-1 mAb (clone RMP1-14) into A/J mice every 3 days for 21 days. Control mice were treated with rat immunoglobulin G2a (IgG2a) isotype Abs. We found that the αPD-1 mAb treatment led to inflammation in multiple organs such as the heart, lung, colon, skeletal muscle, and pancreas by histologic analysis, while isotype controls showed no significant inflammation in all tested organs (Figure 1A). The incidence of autoimmune inflammation by PD-1 blockade differed between organs, ranging from 19% in the heart to 53% in the colon (Figure 1B; Table S1). Most mice with cardiac infiltration simultaneously developed autoimmune inflammation in other organs (Table S1). No significant infiltrations were noted in the thyroid, kidney, and ankle joint of mice treated with αPD-1 mAb or isotype control. In the blood, we found that PD-1 blockade led to a reduction in $CD62L^+CD44^-$ naive subset with a corresponding increase of the $CD62L^+CD44^+$ memory subset in $CD8^+$ T cells compared with isotype control (Figures 1C and 1D). The proportion of the $CD62L^-CD44^+$ effector $CD8^+$ T cell subset was also increased in αPD-1 mAb-treated mice but was not significant (Figure S1A). Peripheral $CD4^+$ T cells had increased proportions of $CD62L^+CD44^+$ memory cells in the PD-1 blockade group, while naive and effector $CD4^+$ T cells were comparable between αPD-1

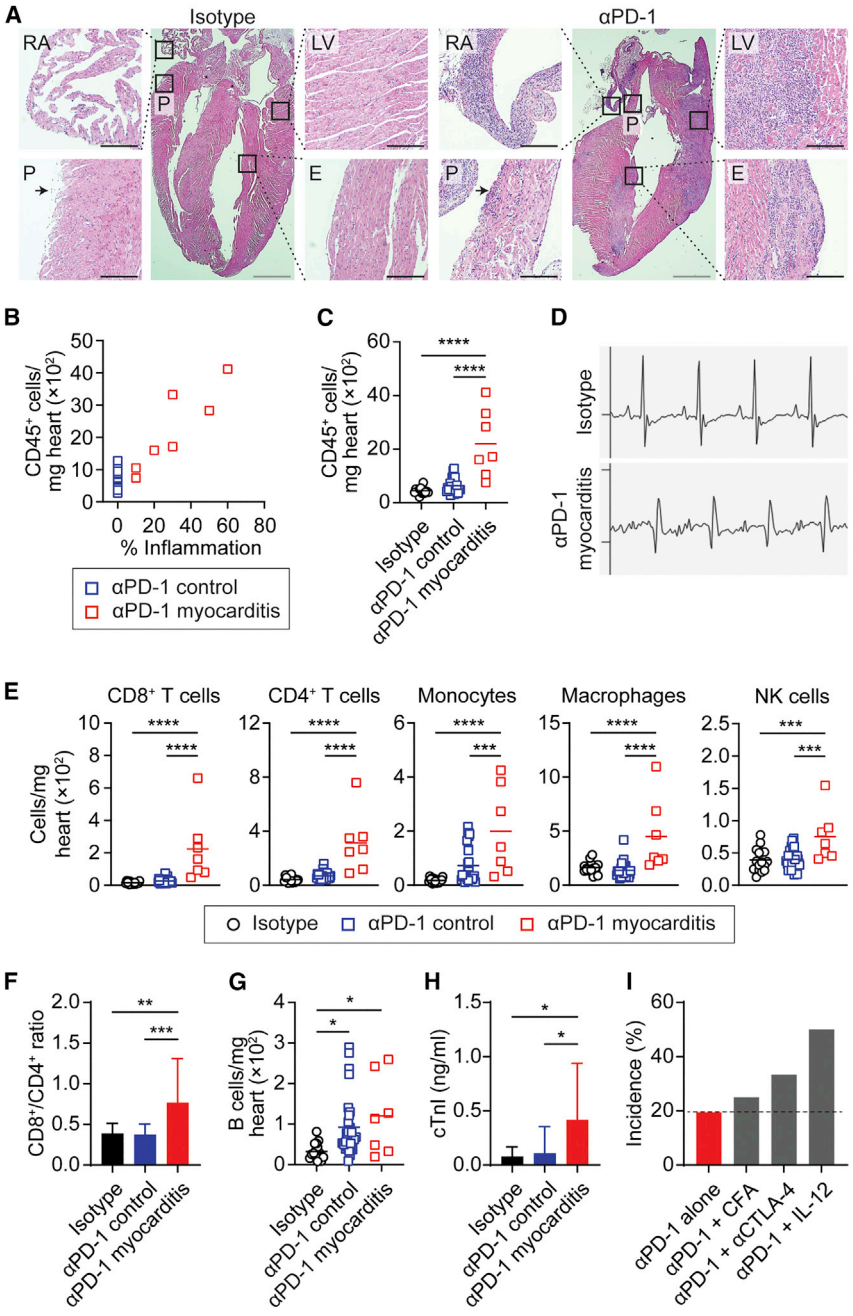

Figure 2. αPD-1 mAb treatment causes ICI-associated myocarditis in mice

(A) Representative images of H&E staining on right atrium (RA), left ventricle (LV), pericardium (P), and endocardium (E) from αPD-1 mAb-treated A/J mice and isotype controls. Arrows indicate P. Scale bars: 100 (black) or 800 μm (gray).

(B and C) Myocarditis development assessed by histology (B) and flow cytometry analysis (B and C). αPD-1 mAb-treated mice were divided into two subgroups by histologic observation—myocarditis development (αPD-1 myocarditis) and no myocarditis (αPD-1 control). Number of $CD45^+$ infiltrating cells in hearts was assessed by flow cytometry.

(D) Electrocardiogram trace of mice with αPD-1 myocarditis and isotype controls.

(E) Number of cardiac $CD8^+$ T cells ($CD3^+CD8^+$), $CD4^+$ T cells ($CD3^+CD4^+$), monocytes ($CD11b^+Ly6G^-F4/80^+Ly6C^+$), macrophages ($CD11b^+Ly6G^-F4/80^+CD64^+Ly6C^-$), and NK cells ($NKp46^+$) in αPD-1 myocarditis, αPD-1 control, and isotype control mice.

(F) Ratio of $CD8^+$ T cells to $CD4^+$ T cells in hearts of αPD-1 myocarditis, αPD-1 control, and isotype control mice.

(G) Number of B cells ($CD19^+$) in mouse hearts of αPD-1 myocarditis, αPD-1 control, and isotype control groups.

(H) Serum cTnI levels in αPD-1 myocarditis, αPD-1 control, and isotype control mice.

(I) Incidence of myocarditis in mice treated with αPD-1 mAb alone or in combination with CFA, αCTLA-4 mAb, or IL-12.

Pooled data of two or three experiments are shown. One-way ANOVA with Tukey's test was used for statistical analysis. *p < 0.05; **p < 0.005; ***p < 0.0005; ****p < 0.0001.

mAb and isotype controls (Figures 1C, 1E, and S1B). These results indicate that PD-1 inhibitor treatment can lead to multiorgan irAEs associated with activated T cells in mice.

PD-1 blockade leads to ICI-associated myocarditis development in mice

Several reports have shown that patients with ICI-associated myocarditis had elevated cTnI levels, arrhythmia, and cardiac infiltration of T cells and $CD68^+$ myeloid cells.[7,8,11,12,14] Thus, we investigated whether myocarditis resulting from PD-1 inhibitor treatment in mice recapitulates human ICI-associated myocarditis. Myocarditic mice had mild to severe infiltrations throughout the entire heart including the ventricle, atrium, pericardium, and endocardium (Figure 2A). For further examination, we divided αPD-1 mAb-treated mice into two subgroups—mice with or without myocarditis development, hereafter called αPD-1 myocarditis and αPD-1 control, respectively (Figure 2B). Myocarditis development and severity were assessed by histological analysis (Figure 2B). Flow cytometry analysis confirmed a significant increase of infiltrating $CD45^+$ cells in the hearts with αPD-1 myocarditis compared with isotype and αPD-1 control groups (Figure 2C). Furthermore, in the αPD-1 myocarditis group, three mice with the most cardiac $CD45^+$ cell numbers exhibited an abnormal ECG trace, while all isotype and αPD-1 control mice preserved normal electrical activity (Figure 2D). The flow cytometry analysis revealed a significantly higher number of $CD8^+$ T cells, $CD4^+$ T cells, monocytes, macrophages, and natural killer (NK) cells in the hearts with αPD-1 myocarditis than those of other groups (Figure 2E). The ratio of $CD8^+$ to $CD4^+$ T cells was also increased in the hearts with

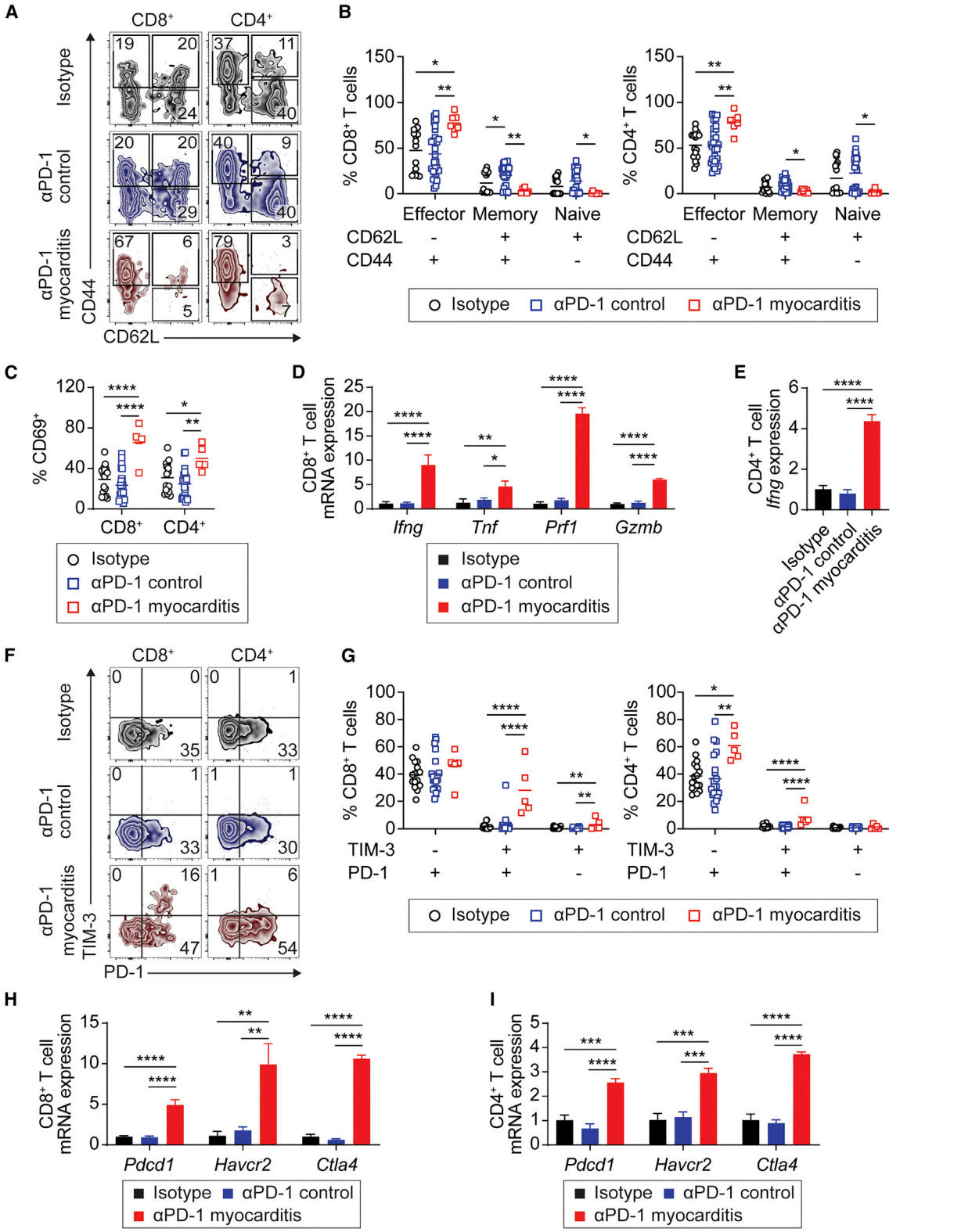

(legend on next page)

αPD-1 myocarditis compared with isotype and αPD-1 controls, suggesting the predominance of $CD8^+$ T cells during PD-1 inhibitor-induced myocarditis (Figure 2F). Cardiac B cell number was increased after PD-1 inhibitor treatment regardless of myocarditis development compared with the isotype control (Figure 2G). The number of γδ T cells and neutrophils was comparable between all groups (Figure S2A). Elevated serum cTnI levels suggested cardiac damage in mice with αPD-1 myocarditis, confirmed by increased apoptotic cardiomyocytes in the TUNEL assay (Figures 2H and S2B). Next, to test if the incidence of PD-1 inhibitor-induced myocarditis can be increased by supplementation with adjuvant or other immunotherapy, we treated mice with complete Freund's adjuvant (CFA), αCTLA-4 mAb (clone UC-10-4F10-11), or recombinant interleukin (IL)-12p70, in addition to αPD-1 mAb. All tested supplements raised the incidence of myocarditis induced by PD-1 blockade, and IL-12 was the most potent among them (Figure 2I). Without PD-1 inhibitor treatment, recombinant IL-12 alone was sufficient to induce a mild level of myocarditis in mice at the incidence of 20%, while mice treated with CFA or αCTLA-4 mAb alone did not develop myocarditis (Figure S2C). To determine if this model can be used in other immunocompetent mouse strains, we treated C57BL/6 and BALB/c mice with αPD-1 mAb for 21 days. Unlike A/J mice, those mice did not exhibit significant myocarditis development. Collectively, our findings indicate that αPD-1 mAb treatment causes myocarditis development in A/J mice, recapitulating human ICI-associated myocarditis.

Cardiac T cells are highly activated during PD-1 inhibitor-induced myocarditis

As shown in Figure 2E, mice with PD-1 inhibitor-induced myocarditis showed increased numbers of both $CD8^+$ and $CD4^+$ T cells in the hearts compared with other groups. We tested if cardiac T cells exhibit an activated and pathogenic phenotype and gene-expression profile in mice with αPD-1 myocarditis. $CD62L^-CD44^+$ effector cell subsets of both $CD8^+$ and $CD4^+$ T cells in the αPD-1 myocarditis group were proportionally increased compared with isotype and αPD-1 controls (Figures 3A and 3B). Similarly, the absolute number of effector $CD8^+$ and $CD4^+$ T cells was significantly increased in mice with αPD-1 myocarditis (Figure S3A). In addition, we found that CD69 expression, an activation marker, on cardiac T cells was upregulated in mice with αPD-1 myocarditis (Figure 3C). Gene-expression profiles revealed that cardiac $CD8^+$ T cells in the αPD-1 myocarditis group expressed a higher level of *Ifng* (interferon [IFN]-γ), *Tnf* (tumor necrosis factor [TNF]-α), *Prf1* (perforin), and *Gzmb* (granzyme B) than that of isotype and αPD-1 controls (Figure 3D). Similarly, $CD4^+$ T cells in the hearts with αPD-1 myocarditis showed upregulated *Ifng* mRNA expression (Figure 3E). It is well known that highly activated T cells express immune checkpoint molecules such as CTLA-4 and PD-1 as compensatory regulation.[32] We examined the expression of immune checkpoint molecules on cardiac T cells by flow cytometry. Cardiac $CD8^+$ T cells expressing both TIM-3 and PD-1 or only TIM-3 were increased in mice with αPD-1 myocarditis compared with isotype and αPD-1 controls (Figures 3F and 3G). Cell frequency of PD-1 single-positive $CD8^+$ T cells was comparable between groups (Figures 3F and 3G). In comparison, cardiac $CD4^+$ T cells revealed an increase of subsets expressing both TIM-3 and PD-1 or only PD-1 compared with other groups (Figures 3F and 3G). There was no proportional difference in $TIM3^+PD\text{-}1^-$ $CD4^+$ T cells between groups (Figures 3F and 3G). The absolute number of all $CD8^+$ and $CD4^+$ subpopulations—$TIM\text{-}3^-PD\text{-}1^+$, $TIM\text{-}3^+PD\text{-}1^+$, and $TIM\text{-}3^+PD\text{-}1^-$—was significantly increased in the αPD-1 myocarditis group compared with isotype and αPD-1 controls (Figure S3B). Supportively, we found that cardiac T cell expression of immune checkpoint transcripts such as *Pdcd1* (PD-1), *Havcr2* (TIM-3), and *Ctla4* (CTLA-4) was significantly upregulated in mice with αPD-1 myocarditis compared with other groups (Figures 3H and 3I). These data suggest that PD-1 blockade can activate pathogenic T cells in the heart, leading to the development of myocarditis.

Cardiac-myosin-specific T cells are associated with PD-1 inhibitor-induced myocarditis

Cardiac myosin is one of the autoantigens related to myocarditis onset and progress in humans and mice.[24,25,28–31] To test if T cell autoimmunity against cardiac antigens contributes to ICI-associated myocarditis, we searched for cardiac-myosin-specific T cells in the heart with αPD-1 myocarditis using α-myosin heavy chain (Myhc) peptide-major histocompatibility complex (MHC) tetramers. $CD8^+$ T cells and $CD4^+$ T cells were stained with $Myhc_{338\text{-}348}$-MHC class I tetramers and $Myhc_{334\text{-}352}$-MHC class II tetramers, respectively.[31,33,34] In the hearts with αPD-1 myocarditis, the number of cardiac-myosin-specific autoimmune $CD8^+$ and $CD4^+$ T cells was significantly increased compared with isotype and αPD-1 control groups (Figures 4A and 4B). Cardiac-myosin-specific and bystander T cells in the αPD-1 myocarditis group showed an activated phenotype ($CD62^-CD44^+CD69^+$) at a comparable level; however, transcript profiles revealed that cardiac-myosin-specific $CD8^+$ T cells

Figure 3. Cardiac T cells are activated in mice with PD-1 inhibitor-induced myocarditis

(A and B) Flow cytometry analysis (A) and cell frequencies (B) of effector ($CD62L^-CD44^+$), memory ($CD62L^+CD44^+$), and naive ($CD62L^+CD44^-$) cells in cardiac $CD8^+$ and $CD4^+$ T cells from αPD-1 mAb-treated mice and isotype controls. αPD-1 mAb-treated mice were divided into two subgroups—myocarditis development (αPD-1 myocarditis) and no myocarditis (αPD-1 control).

(C) Cell frequency of $CD69^+$ T cells in hearts of αPD-1 myocarditis, αPD-1 control, and isotype control mice.

(D and E) Gene expression of cardiac $CD8^+$ (D) and $CD4^+$ (E) T cells in αPD-1 myocarditis, αPD-1 control, and isotype control groups. $CD8^+$ and $CD4^+$ T cells were fluorescence-activated cell sorted (FACS) from heart cells.

(F and G) Flow cytometry analysis (F) and cell frequencies (G) of $TIM\text{-}3^-PD\text{-}1^+$, $TIM\text{-}3^+PD\text{-}1^+$, and $TIM\text{-}3^+PD\text{-}1^-$ cells in $CD8^+$ and $CD4^+$ T cells from hearts of αPD-1 myocarditis, αPD-1 control, and isotype control mice.

(H and I) Gene expression of FACS cardiac $CD8^+$ (H) and $CD4^+$ (I) T cells from αPD-1 myocarditis, αPD-1 control, and isotype control mice.

Pooled data of two or three experiments are shown in (A)–(C), (F), and (G). Representative data of two independent experiments are shown as mean values in (D), (E), (H), and (I). One-way ANOVA with Tukey's test was used for statistical analysis. *$p < 0.05$; **$p < 0.005$; ***$p < 0.0005$; ****$p < 0.0001$.

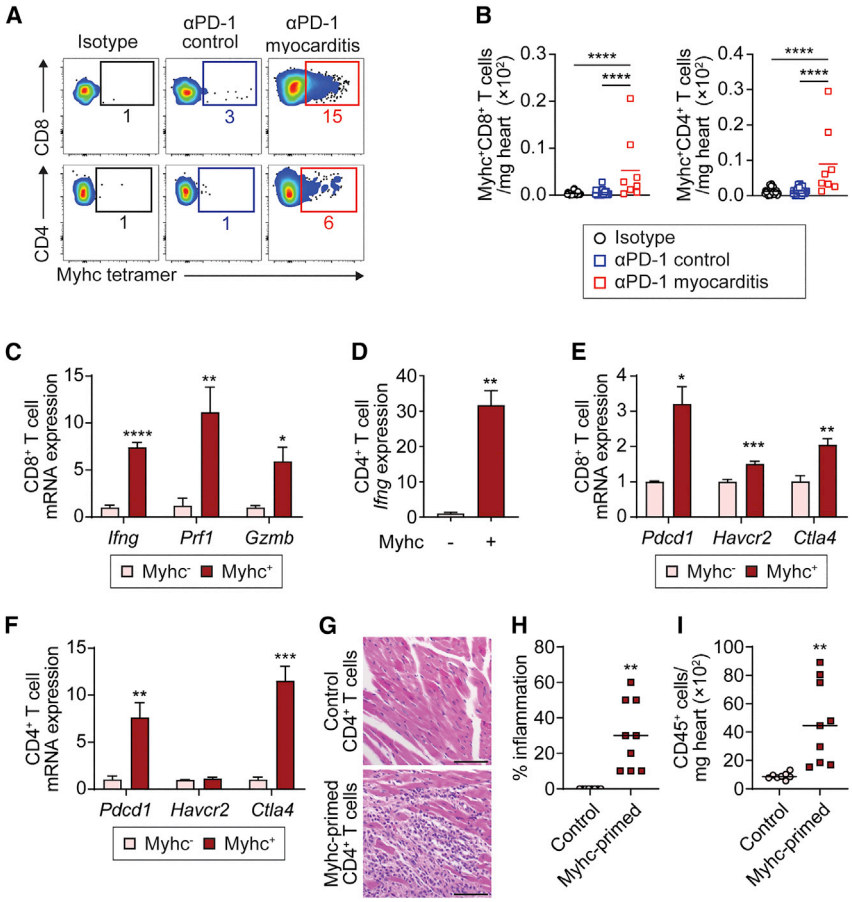

Figure 4. T cells specific for cardiac myosin contribute to PD-1 inhibitor-induced myocarditis

(A and B) Flow cytometry analysis (A) and cell frequencies (B) of cardiac myosin-MHC tetramer-positive cells in $CD8^+$ and $CD4^+$ T cells of αPD-1 mAb-treated A/J mouse hearts and isotype controls. αPD-1 mAb-treated mice were divided into two subgroups—myocarditis development (αPD-1 myocarditis) and no myocarditis (αPD-1 control). $CD8^+$ and $CD4^+$ T cells were stained with $Myhc_{338-348}$-H-$2D^d$ and $Myhc_{334-352}$-I-A^k tetramers, respectively.

(C–F) Gene expression of cardiac-myosin-specific T cells in mice with αPD-1 myocarditis. Myhc tetramer-positive and -negative cells were FACS from cardiac $CD8^+$ (C and E) and $CD4^+$ (D and F) T cells.

(G) Representative images of H&E staining on hearts from mice received Myhc-primed or control $CD4^+$ donor T cells. All recipients were treated with αPD-1 mAb after T cell transfer. Scale bars: 50 μm.

(H) Percentage of inflamed area in heart section from mice received Myhc-primed or control $CD4^+$ donor T cells.

(I) Number of $CD45^+$ infiltrating cells in hearts assessed by flow cytometry analysis.

Pooled data of two or three experiments are shown in (A), (B), and (G)–(I). Representative data of two independent experiments are shown as mean values in (C)–(F). One-way ANOVA with Tukey's test (B) or Student's t test (C–F, H, and I) was used for statistical analysis. *$p < 0.05$; **$p < 0.005$; ***$p < 0.0005$; ****$p < 0.0001$.

expressed a higher level of *Ifng*, *Prf1*, and *Gzmb* genes than that of bystander T cells during αPD-1 myocarditis (Figure 4C). Myosin-specific $CD4^+$ T cells also showed elevated *Ifng* expression (Figure 4D). Additionally, we found that genes related to immune checkpoint molecules such as *Pdcd1*, *Havcr2*, and *Ctla4* were upregulated in cardiac-myosin-specific autoimmune $CD8^+$ T cells compared with non-myosin-specific bystander T cells (Figure 4E). Cardiac-myosin-specific $CD4^+$ T cells showed an increased mRNA expression level of *Pdcd1* and *Ctla4* but not for the *Havcr2* gene (Figure 4F). To confirm the pathogenicity of myosin-specific T cells in myocarditis, we adoptively transferred myosin peptide-primed T cells into sublethally irradiated mice that were treated with αPD-1 mAb after the transfer. Myosin-primed $CD4^+$ T cell donors were isolated from spleens of mice immunized with $Myhc_{334-352}$ peptide, while control $CD4^+$ T cell donors were isolated from naive mouse spleens. Both myosin-primed T cells and control T cells were pulsed with $Myhc_{334-352}$ peptide *in vitro* and adoptively transferred to the recipients. Using the histologic and flow cytometric analyses, we found that all mice that received myosin-pulsed $CD4^+$ T cells developed myocarditis 18 days after the adoptive transfer (Figures 4G, 4H, 4I, and S4A). The number of cardiac $CD4^+$ T cells, monocytes, and macrophages was significantly increased in the recipients of myosin-primed $CD4^+$ T cells compared with the control group (Figure S4B). In contrast, no recipients in the control T cell group developed myocarditis. Honjo and his colleagues have previously reported that PD-1-deficient BALB/c mice spontaneously developed inflammatory dilated cardiomyopathy mediated by anti-cTnI autoantibodies.[22,23] In our mice with αPD-1 myocarditis, the serum level of anti-cTnI or cardiac myosin Abs was comparable or slightly elevated compared with the isotype and αPD-1 control groups, suggesting a limited role of anti-heart antigen autoantibodies in αPD-1 myocarditis (Figure S4C). Collectively, PD-1 inhibitor treatment leads to the activation of autoimmune T cells specific for cardiac myosin during ICI-associated myocarditis.

PD-1-expressing cardiac-myosin-specific T cells are present in naive mice

To understand how PD-1 inhibitor treatment initiates the development of myocarditis, we examined the presence of cardiac-myosin-specific autoimmune T cells and their PD-1 expression in naive mice. We found that 1%–2% of $CD8^+$ and $CD4^+$ T cells in the naive heart, mediastinal lymph node (medLN), and spleen exhibited a specificity to cardiac myosin (Figures 5A, 5B, and S5A). In all tested organs, cardiac-myosin-specific $CD4^+$ T cells expressed a higher level of PD-1 compared with non-myosin-specific T cells (Figures 5C and 5D). Within the myosin-specific $CD4^+$ T cells of naive organs, PD-1-expressing cells showed a greater proportion of

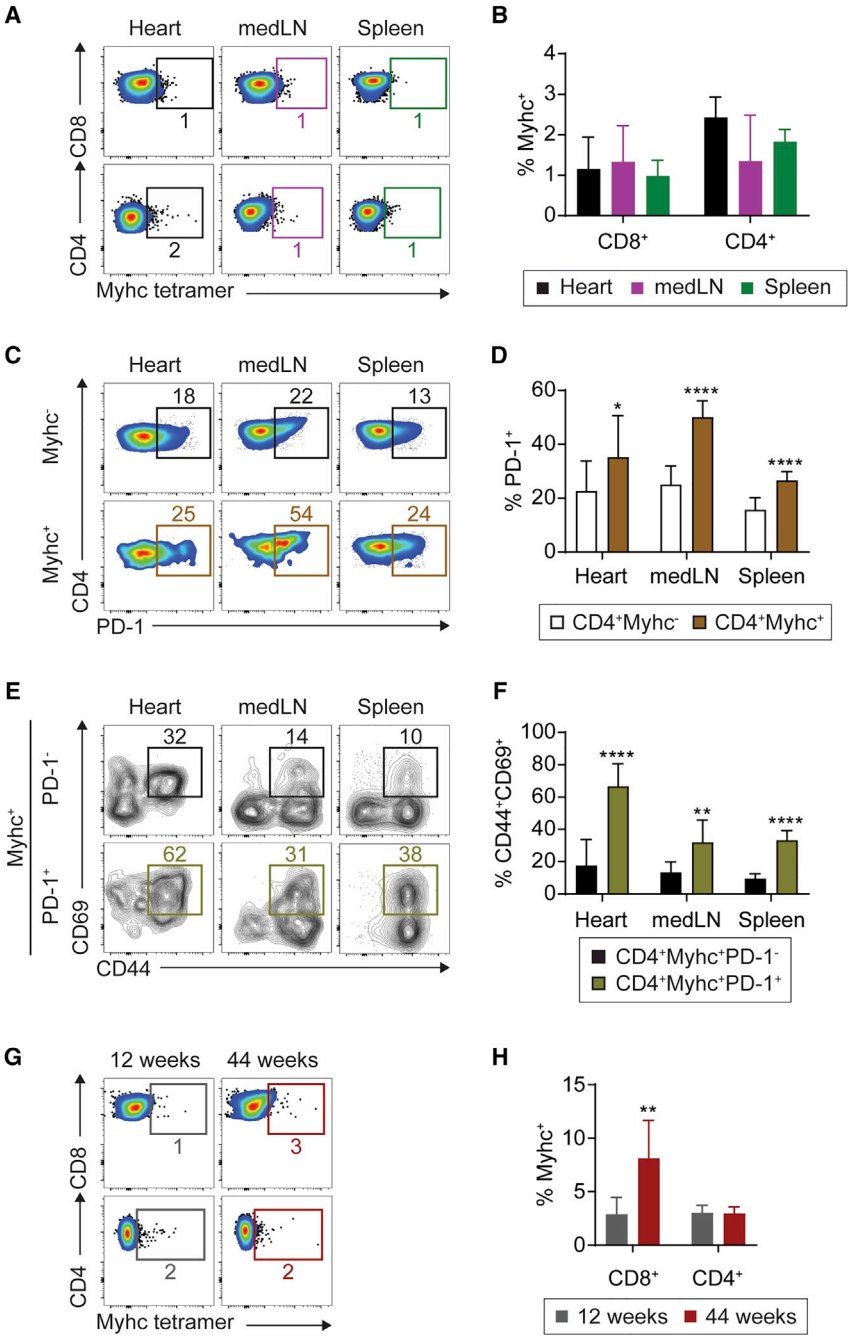

Figure 5. PD-1-expressing cardiac myosin-specific T cells exist in naive A/J mice

(A and B) Flow cytometry analysis (A) and cell frequencies (B) of cardiac myosin-MHC tetramer-positive cells in $CD8^+$ and $CD4^+$ T cells of naive A/J mice. Hearts, mediastinal lymph nodes (medLNs), and spleens were examined. $CD8^+$ and $CD4^+$ T cells were stained with $Myhc_{338-348}$-H-$2D^d$ and $Myhc_{334-352}$-I-A^k tetramers, respectively.

(C and D) Flow cytometry plots (C) and frequencies (D) of PD-1-expressing cells in $Myhc_{334-352}$ tetramer-positive and -negative $CD4^+$ T cells. Cells were isolated from naive mouse hearts, medLNs, and spleens.

(E and F) Flow cytometry analysis (E) and cell frequencies (F) of $CD44^+CD69^+$ cells in PD-1-positive and -negative cardiac-myosin-specific $CD4^+$ T cells. Cells were isolated from naive hearts, medLNs, and spleens.

(G and H) Flow cytometry plots (G) and cell frequencies (H) of cardiac myosin-MHC tetramer-positive cells among $CD8^+$ and $CD4^+$ T cells in the heart of naive young (12 weeks) and aged (44 weeks) mice.

Pooled data of two experiments are shown. Student's t test was used for statistical analysis. $^*p < 0.05$; $^{**}p < 0.005$; $^{****}p < 0.0001$.

effector- or memory-like phenotype ($CD44^+CD69^+$) compared with the PD-1^- counterpart, suggesting their quick response to PD-1 inhibitor treatment (Figures 5E and 5F). In the $CD8^+$ T cells in the heart and medLN, the PD-1 expression level was comparable between cardiac-myosin-specific and non-myosin-specific cells, while cardiac-myosin-specific $CD8^+$ T cells in the spleen showed a higher PD-1 expression than their non-myosin-specific counterpart (Figures S5B and S5C). However, PD-1^+ cardiac-myosin-specific $CD8^+$ T cells showed an increased $CD44^+CD69^+$ compartment compared with PD-1^- myosin-specific cells (Figures S5D and S5E). To study the factors affecting the number of myosin-specific autoimmune T cells, we compared cardiac T cell profiles in aged or female mice with young adult males. First, we found that naive aged mice had a significantly higher number of myosin-specific $CD8^+$ T cells in the heart compared with young adults, while myosin-specific $CD4^+$ T cells were comparable between aged and young mice (Figures 5G and 5H). In the spleen, aged and young mice had a comparable number of myosin-specific $CD8^+$ T cells. Second, male and female mice showed no differences in the number of both $CD8^+$ and $CD4^+$ myosin-specific autoimmune T cells in the heart (Figure S5F). In addition, we found that cardiac-myosin-specific $CD8^+$ and $CD4^+$ T cells were present in the blood of naive mice as well as in the heart, medLN, and spleen. To investigate whether the number of circulating myosin-specific T cells is associated with PD-1 inhibitor-induced myocarditis development, we collected blood T cells prior to αPD-1 mAb treatment. In the retrospective analysis after 21 days of PD-1 blockade, the number of circulating myosin-specific T cells in the αPD-1 myocarditis group showed no differences from the isotype or αPD-1 control group (Figure S5G). These data suggest that cardiac-myosin-specific autoimmune T cells are present in the naive heart or other organs and can be rapidly activated upon PD-1 inhibitor treatment.

DISCUSSION

In this study, we established a mouse model for ICI-associated myocarditis and showed cardiac-myosin-specific autoreactive T cells to be an important mediator. 19% of A/J mice injected with PD-1 inhibitor developed myocarditis as assessed by histology and flow cytometry analysis, showing serum cTnI level elevation and ECG abnormality similar to human ICI-associated myocarditis. We also found the predominance of $CD8^+$ T cells over $CD4^+$ T cells in cardiac inflammatory cells of mice with myocarditis. We administrated αPD-1 mAb (clone RMP1-14) into A/J mice with no additional procedures such as immunization, viral infection, or tumor cell inoculation. By far, no mouse models for spontaneous development of ICI-associated myocarditis induced by PD-1 inhibitor alone in an immunocompetent mouse strain have been reported. In a recent study, PD-1 inhibitor treatment induced myocardial T cell infiltration and cardiac dysfunction in C57BL/6 mice bearing tumors.[35] However, those mice showed no signs of local T cell accumulation and cardiomyocyte death, indicating a milder severity of myocarditis than that of our model. A/J mice are widely used to investigate the pathogenesis of autoimmune or viral myocarditis.[29,36–39] Aged A/J mice are known to develop skeletal muscle dystrophy, hearing loss, and cancer spontaneously, but autoimmune inflammation in the heart or other organs has not been reported.[40–42] We used 8- to 12-week-old and 44-week-old mice that showed no cancer development in any organs after αPD-1 mAb treatment or isotype controls.

Besides myocarditis, we found that PD-1 inhibitor treatment caused irAEs in various organs. It has been reported that mice with PD-1 blockade using neutralizing Abs or genetic manipulation developed autoimmune inflammation in the lung, colon, and pancreas.[43–45] However, these mice were on an MRL or NOD background that is predisposed to autoimmune disorders and are not considered an immunocompetent strain. Thus, our approach of inducing myocarditis development using PD-1 inhibitor treatment in A/J mice can be a clinically relevant animal model for human ICI-associated myocarditis and potentially other irAEs including pneumonia, colitis, myositis, and pancreatitis. In addition, our αPD-1 mAb treatment approach has an advantage over the genetic deletion of PD-1 expression, avoiding further manipulations during the developmental stage. CTLA-4-deficient mice died of lethal myocarditis and pancreatitis by 3–4 weeks of age; however, conditional CTLA-4 ablation in mature adult mice using a tamoxifen-inducible Cre system was not lethal.[46,47] The adult mice conditionally lacking CTLA-4 expression developed autoimmune inflammation in the heart and pancreas, but its incidence and severity were lower than those of congenital *CTLA-4*$^{-/-}$ mice.[47]

The mechanism of ICI-associated myocarditis onset and progress is unclear. In an early case report of ICI-associated myocarditis, melanoma patients treated with ipilimumab, a CTLA-4 inhibitor, and nivolumab, a PD-1 inhibitor, presented an expansion of shared T cell clones in the myocardium and tumor, suggesting the contribution of T cells targeting both heart and tumor antigens to myocarditis development.[14] However, it has not been addressed which antigens are responsible for activating pathogenic T cells in ICI-associated myocarditis and where they originate—the heart or tumor. In our study, PD-1 inhibitor treatment alone was sufficient to induce myocarditis development in mice and did not require tumor cells. This indicates that autoreactive T cells targeting cardiac antigens, rather than tumor antigens, could play a crucial role in ICI-associated myocarditis. Using the tetramer staining assay, we found that cardiac myosin was a target of highly activated pathogenic T cells in mice with PD-1 inhibitor-induced myocarditis. Immunization with myosin purified from mouse hearts or its shortened peptide is a well-established method to induce autoimmune myocarditis in various mouse strains.[38] Mice with CVB3 infection-induced myocarditis also revealed increased anti-cardiac myosin Ab levels in the serum and generation of myosin-specific T cells in the spleen and lymph nodes.[48,49] In our current study, we showed that the adoptive transfer of cardiac-myosin-pulsed $CD4^+$ T cells caused acute myocarditis development in mice, as we previously have shown.[50] Supportively, it has been reported that transgenic mice expressing T cell receptors specific for cardiac myosin developed spontaneous myocarditis between 2 and 6 weeks of age.[51] Given the elevated level of anti-cardiac myosin autoantibody in patients with acute myocarditis and its sequela dilated cardiomyopathy, the autoimmune response against cardiac myosin is proposed as an important mechanism of community-acquired myocarditis.[52,53] Thus, cardiac-myosin-specific autoimmune T cells might be a potential mediator in ICI-associated myocarditis.

Activated T cells express immune checkpoint molecules including PD-1 and CTLA-4 to induce T cell exhaustion in the periphery as a negative regulatory mechanism.[32] In our mouse model for ICI-associated myocarditis, PD-1 neutralizing mAb treatment might block inhibitory signaling in cardiac-myosin-specific autoimmune T cells, causing persistent T cell activation shown by highly upregulated cytokine and immune checkpoint molecule expression. PD-L1, a ligand for PD-1, is expressed by both hematopoietic and non-hematopoietic cells.[2] In the mouse heart, cardiomyocytes and endothelial cells express PD-L1 to protect from pathogenic T cell immune responses.[17,43,54] We have previously reported that loss of graft endothelial PD-L1 expression was significantly associated with $CD8^+$ T cell infiltration in patients with heart transplantation.[55] Similar to the PD-1 inhibitor, PD-L1 inhibitor treatment has led to ICI-associated myocarditis in patients with cancer.[56,57]

Given that IL-12 supplementation increased the incidence of PD-1 inhibitor-induced myocarditis in our study, IL-12 could play an important role in the pathogenesis of ICI-associated myocarditis. Other animal studies showed that IL-12 receptor signaling was required for the initiation and progress of autoimmune and viral myocarditis.[58–61] As a suggested mechanism, IL-12 enhanced the differentiation of pathogenic effector $CD8^+$ T cells causing lethal myocarditis when adoptively transferred into mice.[62] In both clinical and preclinical settings, anti-tumor T cell activity induced by PD-1 blockade became more effective when combined with IL-12 treatment.[63,64]

To address how ICI treatment is involved in myocarditis onset, we first sought cardiac-myosin-specific T cells in naive A/J mice. Our tetramer assay showed that myosin-specific T cells were present in naive mouse heart, medLN, and spleen. This is supported by the finding that autoreactive T cells recognizing

cardiac myosin avoided the negative selection during the thymic developmental stage in mice and humans due to a lack of Myhc gene (*Myh6*) expression in medullary thymic epithelial cells.[65] Second, we found that there was a PD-1-expressing subpopulation among cardiac-myosin-specific autoimmune T cells in naive mouse tissues. A proportion of those PD-1$^+$ cardiac-myosin-specific T cells exhibited a phenotype of CD44 and CD69 co-expression. PD-1, CD44, and CD69 are well-known activation markers expressed in effector, central memory, or tissue-resident memory T cells, which have already been exposed to antigens.[66–68] Taken together, we suggest that PD-1 inhibitor treatment may re-activate cardiac-myosin-experienced T cells by blocking the regulatory signaling, leading to ICI-associated myocarditis development. Further investigation using a high-dimensional single-cell analysis is needed to identify and comprehensively characterize autoimmune T cells recognizing heart antigens.

The determinant of ICI-associated myocarditis onset and progress is also unclear. Our study showed that only a small subgroup of A/J mice developed myocarditis. In humans, the incidence of ICI-associated myocarditis is about 1% among patients with cancer treated with ICIs.[15] In our mouse model, the number of most cardiac immune cell populations including myosin-specific T cells was increased only in the αPD-1 myocarditis group, but not in the αPD-1 control group, compared with the isotype control group. This suggests that ICI treatment could induce the development of myocarditis only in individuals with a sufficient number of activated cardiac-myosin-specific autoimmune T cells. Some studies have reported molecular mimicry between cardiac myosin and microbes in T cell targets, indicating the highly variable number and characteristics of cardiac-myosin-specific T cells between individuals due to different environmental conditions.[69,70] In this study, we tested only cardiac myosin as an autoantigen responsible for ICI-associated myocarditis development. However, there are other well-known heart antigens such as β1-adrenergic receptor, muscarinic M2 receptor, and Na-K-ATPase, recognized by autoantibodies in patients with myocarditis and dilated cardiomyopathy.[71,72] This suggests that multiple different autoimmune targets could be involved in ICI-associated myocarditis. Meanwhile, most mice with myocarditis in our study developed autoimmune inflammation in other organs at the same time, resembling patients who had two or more irAEs after ICI treatment.[73] This may be explained by the concurrent activation of multiple T cell clones targeting different tissue-specific antigens upon ICI treatment but also by the activation of a single autoimmune T cell clone recognizing a common antigen throughout organs including the heart. In our study, there were αPD-1 mAb-treated mice that did not develop myocarditis but revealed irAEs in one or more other organs, suggesting the independent activation of T cell clones targeting other organs from myosin-specific T cells.

In our study, αPD-1 mAb treatment caused myocarditis development in A/J mice but not in C57BL/6 and BALB/c mice, suggesting that genetic or phenotypic differences between those strains may contribute to the activation of autoreactive T cells in the heart. Despite being considered an immunocompetent strain, A/J mice lack complement C5 expression due to genetic defect, unlike C5-sufficient C57BL/6 and BALB/c mice.[74] The C5 deficiency in A/J mice led to a higher susceptibility to *Mycobacterium tuberculosis* or *Listeria monocytogenes* infection compared with C57BL/6 mice.[75,76] In addition, the MHC haplotype expressed in A/J mice is H-2^a, different from that of C57BL/6 (H-2^b) and BALB/c (H-2^d) mice. The human leukocyte antigen (HLA) polymorphism has been suggested as a genetic risk associated with the pathogenesis of inflammatory dilated cardiomyopathy.[77] Thus, C5 deficiency and MHC haplotype of A/J mice would be associated with increased susceptibility to myocarditis upon PD-1 inhibitor treatment.

Our data revealed that aging affected the increased number of myosin-specific CD8$^+$ T cells in the heart, suggesting a higher risk of PD-1 inhibitor-related myocarditis in the elderly. This is supported by a report describing an increased risk of ICI-associated myocarditis in patients aged 75 years or older.[78] However, unlike in the heart, the number of myosin-specific CD8$^+$ T cells in aged mouse spleen was not increased, indicating that peripheral T cells may not reflect the autoreactive T cell context of the heart. Our retrospective analysis revealed that mice with αPD-1 mAb-induced myocarditis had no outstanding myosin-specific T cell counts in the circulation compared with control mice before αPD-1 mAb treatment. Thus, the anatomic distribution of myosin-specific autoimmune T cells could be an important factor contributing to ICI-associated myocarditis as well as senescence. Meanwhile, in many autoimmune diseases, the activation of the innate immune system is considered to trigger the disease, driving further activation of adaptive immunity.[79] Interestingly, PD-1 can be expressed in innate immune cells such as macrophages, dendritic cells, and innate lymphoid cells during diseased conditions, playing a regulatory role.[80–82] Macrophages and monocytes were a predominant population in cardiac infiltration of our mouse model and patients with ICI-associated myocarditis, suggesting the pathogenic activation of the innate immune system directly by ICI treatment as well as T cell activation.[11,12,14] In this study, the crucial role of autoreactive T cells, a part of the adaptive immune system, in ICI-associated myocarditis was shown using PD-1 inhibitor treatment and adoptive T cell transfer approaches. More studies will be necessary to address the role of innate immunity in ICI-associated myocarditis.

In conclusion, we generated a clinically relevant mouse model for ICI-associated myocarditis by administrating αPD-1 mAb into the A/J mouse strain. Mice with ICI-associated myocarditis showed increased T cells, macrophages, and monocytes in the heart and elevated serum cTnI levels. ECG abnormality was found in mice with very severe ICI-associated myocarditis. αPD-1 mAb-treated mice also developed irAEs in other organs. We found that the number and activity of cardiac-myosin-specific T cells were increased in mice with αPD-1 mAb-induced myocarditis, indicating a contribution of heart autoantigen-reactive T cells to ICI-associated myocarditis. In addition, the presence of PD-1$^+$ cardiac myosin-specific T cells in naive mice suggests that ICI treatment could re-activate heart autoantigen-experienced T cells, which are under control by the PD-1/PD-L1 pathway in naive conditions, leading to myocarditis development.

Limitations of the study

In this study, mice were treated with αPD-1 or isotype mAb for 21 days. No earlier or later time points were tested, limiting the

understanding of the entire time course of ICI-associated myocarditis in our model. The contribution of tumor cells to ICI-associated myocarditis was not tested in our study because there are no syngeneic tumor cell lines available for A/J mice. In the adoptive transfer experiment, we used T cells isolated from myosin peptide-immunized mice as a donor, resulting in myocarditis development in all recipients. Myosin-specific T cells directly sorted from naive mice using tetramer staining were also tested for T cell adoptive-transfer-induced myocarditis. Due to the limited cell number, even after *in vitro* expansion, we were only able to adoptively transfer those T cells to three recipient mice, which developed myocarditis with a 33% incidence. This limits our understanding of the pathogenicity of myosin-specific T cells under naive conditions, which are more clinically relevant than in immunization with cardiac myosin peptide. We showed that A/J mice aged 44 weeks had an increased number of myosin-specific autoreactive T cells in the heart; however, myocarditis induction in those old mice by αPD-1 mAb treatment was not conducted due to the limited number of mice.

STAR★METHODS

Detailed methods are provided in the online version of this paper and include the following:

- KEY RESOURCES TABLE
- RESOURCE AVAILABILITY
  - Lead contact
  - Materials availability
  - Data and code availability
- EXPERIMENTAL MODEL AND SUBJECT DETAILS
  - Mice
- METHOD DETAILS
  - Histology study
  - Electrocardiography
  - Single cell isolation
  - Flow cytometry
  - ELISA
  - TUNEL assay
  - Real-time RT-PCR
  - Adoptive transfer of T cells
- QUANTIFICATION AND STATISTICAL ANALYSIS
  - Statistics

SUPPLEMENTAL INFORMATION

Supplemental information can be found online at https://doi.org/10.1016/j.celrep.2022.111611.

ACKNOWLEDGMENTS

This work was supported by the American Heart Association (AHA) 19TPA34910007 and 20TPA35490421, the National Institutes of Health (NIH)/National Heart, Lung, and Blood Institute (NHLBI) R01HL118183 and R01HL136586, and the Global Autoimmune Institute. T.W. is supported by the 2018 Rhett Lundy Memorial Research Fellowship from the Myocarditis Foundation. M.K.W. is funded by the NIH/National Institute of Arthritis and Musculoskeletal and Skin Diseases (NIAMS) F31AR077406. D.M.H. is funded by the NIH/NHLBI F31HL149328. C.M.J. is funded by the AHA Diversity Supplement Award 961456. We thank the NIH Tetramer Core Facility (contract number 75N93020D00005) for providing the tetramers used in this study.

AUTHOR CONTRIBUTIONS

Conceptualization, T.W. and D.C.; methodology, formal analysis, and investigation, T.W., H.M.K., M.K.W., D.M.H., C.M.J., P.D., and M.V.T.; resources, N.L. and J.R.; writing – original draft, T.W. and D.C.; writing – review & editing, T.W., H.M.K., M.K.W., D.M.H., C.M.J., P.D., M.V.T., N.L., J.R., and D.C.; visualization, T.W., H.M.K., M.K.W., D.M.H., C.M.J., P.D., and M.V.T.; supervision, D.C.; funding acquisition, D.C.

DECLARATION OF INTERESTS

The authors declare no competing interests.

INCLUSION AND DIVERSITY

We support inclusive, diverse, and equitable conduct of research.

Received: March 15, 2022
Revised: August 15, 2022
Accepted: October 14, 2022
Published: November 8, 2022

REFERENCES

1. Kraehenbuehl, L., Weng, C.H., Eghbali, S., Wolchok, J.D., and Merghoub, T. (2022). Enhancing immunotherapy in cancer by targeting emerging immunomodulatory pathways. Nat. Rev. Clin. Oncol. *19*, 37–50. https://doi.org/10.1038/s41571-021-00552-7.
2. Bagchi, S., Yuan, R., and Engleman, E.G. (2021). Immune checkpoint inhibitors for the treatment of cancer: clinical impact and mechanisms of response and resistance. Annu. Rev. Pathol. *16*, 223–249. https://doi.org/10.1146/annurev-pathol-042020-042741.
3. Esfahani, K., Elkrief, A., Calabrese, C., Lapointe, R., Hudson, M., Routy, B., Miller, W.H., Jr., and Calabrese, L. (2020). Moving towards personalized treatments of immune-related adverse events. Nat. Rev. Clin. Oncol. *17*, 504–515. https://doi.org/10.1038/s41571-020-0352-8.
4. Martins, F., Sofiya, L., Sykiotis, G.P., Lamine, F., Maillard, M., Fraga, M., Shabafrouz, K., Ribi, C., Cairoli, A., Guex-Crosier, Y., et al. (2019). Adverse effects of immune-checkpoint inhibitors: epidemiology, management and surveillance. Nat. Rev. Clin. Oncol. *16*, 563–580. https://doi.org/10.1038/s41571-019-0218-0.
5. Song, P., Zhang, D., Cui, X., and Zhang, L. (2020). Meta-analysis of immune-related adverse events of immune checkpoint inhibitor therapy in cancer patients. Thorac. Cancer *11*, 2406–2430. https://doi.org/10.1111/1759-7714.13541.
6. Herrmann, J. (2020). Adverse cardiac effects of cancer therapies: cardiotoxicity and arrhythmia. Nat. Rev. Cardiol. *17*, 474–502. https://doi.org/10.1038/s41569-020-0348-1.
7. Waliany, S., Lee, D., Witteles, R.M., Neal, J.W., Nguyen, P., Davis, M.M., Salem, J.E., Wu, S.M., Moslehi, J.J., and Zhu, H. (2021). Immune checkpoint inhibitor cardiotoxicity: understanding basic mechanisms and clinical characteristics and finding a cure. Annu. Rev. Pharmacol. Toxicol. *61*, 113–134. https://doi.org/10.1146/annurev-pharmtox-010919-023451.
8. Lehmann, L.H., Cautela, J., Palaskas, N., Baik, A.H., Meijers, W.C., Allenbach, Y., Alexandre, J., Rassaf, T., Müller, O.J., Aras, M., et al. (2021). Clinical strategy for the diagnosis and treatment of immune checkpoint inhibitor-associated myocarditis: a narrative review. JAMA Cardiol. *6*, 1329–1337. https://doi.org/10.1001/jamacardio.2021.2241.
9. Läubli, H., Balmelli, C., Bossard, M., Pfister, O., Glatz, K., and Zippelius, A. (2015). Acute heart failure due to autoimmune myocarditis under pembrolizumab treatment for metastatic melanoma. J. Immunother. Cancer *3*, 11. https://doi.org/10.1186/s40425-015-0057-1.

10. Heinzerling, L., Ott, P.A., Hodi, F.S., Husain, A.N., Tajmir-Riahi, A., Tawbi, H., Pauschinger, M., Gajewski, T.F., Lipson, E.J., and Luke, J.J. (2016). Cardiotoxicity associated with CTLA4 and PD1 blocking immunotherapy. J. Immunother. Cancer *4*, 50. https://doi.org/10.1186/s40425-016-0152-y.

11. Tadokoro, T., Keshino, E., Makiyama, A., Sasaguri, T., Ohshima, K., Katano, H., and Mohri, M. (2016). Acute lymphocytic myocarditis with anti-PD-1 antibody nivolumab. Circ. Heart Fail. *9*, e003514. https://doi.org/10.1161/CIRCHEARTFAILURE.116.003514.

12. Koelzer, V.H., Rothschild, S.I., Zihler, D., Wicki, A., Willi, B., Willi, N., Voegeli, M., Cathomas, G., Zippelius, A., and Mertz, K.D. (2016). Systemic inflammation in a melanoma patient treated with immune checkpoint inhibitors-an autopsy study. J. Immunother. Cancer *4*, 13. https://doi.org/10.1186/s40425-016-0117-1.

13. Tay, R.Y., Blackley, E., McLean, C., Moore, M., Bergin, P., Gill, S., and Haydon, A. (2017). Successful use of equine anti-thymocyte globulin (ATGAM) for fulminant myocarditis secondary to nivolumab therapy. Br. J. Cancer *117*, 921–924. https://doi.org/10.1038/bjc.2017.253.

14. Johnson, D.B., Balko, J.M., Compton, M.L., Chalkias, S., Gorham, J., Xu, Y., Hicks, M., Puzanov, I., Alexander, M.R., Bloomer, T.L., et al. (2016). Fulminant myocarditis with combination immune checkpoint blockade. N. Engl. J. Med. *375*, 1749–1755. https://doi.org/10.1056/NEJMoa1609214.

15. Moslehi, J., Lichtman, A.H., Sharpe, A.H., Galluzzi, L., and Kitsis, R.N. (2021). Immune checkpoint inhibitor-associated myocarditis: manifestations and mechanisms. J. Clin. Invest. *131*, 145186. https://doi.org/10.1172/JCI145186.

16. Tsuruoka, K., Wakabayashi, S., Morihara, H., Matsunaga, N., Fujisaka, Y., Goto, I., Imagawa, A., and Asahi, M. (2020). Exacerbation of autoimmune myocarditis by an immune checkpoint inhibitor is dependent on its time of administration in mice. Int. J. Cardiol. *313*, 67–75. https://doi.org/10.1016/j.ijcard.2020.04.033.

17. Seko, Y., Yagita, H., Okumura, K., Azuma, M., and Nagai, R. (2007). Roles of programmed death-1 (PD-1)/PD-1 ligands pathway in the development of murine acute myocarditis caused by coxsackievirus B3. Cardiovasc. Res. *75*, 158–167. https://doi.org/10.1016/j.cardiores.2007.03.012.

18. Wang, J., Okazaki, I.M., Yoshida, T., Chikuma, S., Kato, Y., Nakaki, F., Hiai, H., Honjo, T., and Okazaki, T. (2010). PD-1 deficiency results in the development of fatal myocarditis in MRL mice. Int. Immunol. *22*, 443–452. https://doi.org/10.1093/intimm/dxq026.

19. Wei, S.C., Meijers, W.C., Axelrod, M.L., Anang, N.A.A.S., Screever, E.M., Wescott, E.C., Johnson, D.B., Whitley, E., Lehmann, L., Courand, P.Y., et al. (2021). A genetic mouse model recapitulates immune checkpoint inhibitor-associated myocarditis and supports a mechanism-based therapeutic intervention. Cancer Discov. *11*, 614–625. https://doi.org/10.1158/2159-8290.CD-20-0856.

20. Tarrio, M.L., Grabie, N., Bu, D.X., Sharpe, A.H., and Lichtman, A.H. (2012). PD-1 protects against inflammation and myocyte damage in T cell-mediated myocarditis. J. Immunol. *188*, 4876–4884. https://doi.org/10.4049/jimmunol.1200389.

21. Nishimura, H., Nose, M., Hiai, H., Minato, N., and Honjo, T. (1999). Development of lupus-like autoimmune diseases by disruption of the PD-1 gene encoding an ITIM motif-carrying immunoreceptor. Immunity *11*, 141–151. https://doi.org/10.1016/s1074-7613(00)80089-8.

22. Nishimura, H., Okazaki, T., Tanaka, Y., Nakatani, K., Hara, M., Matsumori, A., Sasayama, S., Mizoguchi, A., Hiai, H., Minato, N., and Honjo, T. (2001). Autoimmune dilated cardiomyopathy in PD-1 receptor-deficient mice. Science *291*, 319–322. https://doi.org/10.1126/science.291.5502.319.

23. Okazaki, T., Tanaka, Y., Nishio, R., Mitsuiye, T., Mizoguchi, A., Wang, J., Ishida, M., Hiai, H., Matsumori, A., Minato, N., and Honjo, T. (2003). Autoantibodies against cardiac troponin I are responsible for dilated cardiomyopathy in PD-1-deficient mice. Nat. Med. *9*, 1477–1483. https://doi.org/10.1038/nm955.

24. Lauer, B., Schannwell, M., Kühl, U., Strauer, B.E., and Schultheiss, H.P. (2000). Antimyosin autoantibodies are associated with deterioration of systolic and diastolic left ventricular function in patients with chronic myocarditis. J. Am. Coll. Cardiol. *35*, 11–18. https://doi.org/10.1016/s0735-1097(99)00485-4.

25. Neumann, D.A., Burek, C.L., Baughman, K.L., Rose, N.R., and Herskowitz, A. (1990). Circulating heart-reactive antibodies in patients with myocarditis or cardiomyopathy. J. Am. Coll. Cardiol. *16*, 839–846. https://doi.org/10.1016/s0735-1097(10)80331-6.

26. Mascaro-Blanco, A., Alvarez, K., Yu, X., Lindenfeld, J., Olansky, L., Lyons, T., Duvall, D., Heuser, J.S., Gosmanova, A., Rubenstein, C.J., et al. (2008). Consequences of unlocking the cardiac myosin molecule in human myocarditis and cardiomyopathies. Autoimmunity *41*, 442–453. https://doi.org/10.1080/08916930802031579.

27. Fairweather, D., Petri, M.A., Coronado, M.J., and Cooper, L.T. (2012). Autoimmune heart disease: role of sex hormones and autoantibodies in disease pathogenesis. Expert Rev. Clin. Immunol. *8*, 269–284. https://doi.org/10.1586/eci.12.10.

28. Myers, J.M., Cooper, L.T., Kem, D.C., Stavrakis, S., Kosanke, S.D., Shevach, E.M., Fairweather, D., Stoner, J.A., Cox, C.J., and Cunningham, M.W. (2016). Cardiac myosin-Th17 responses promote heart failure in human myocarditis. JCI Insight *1*, 85851. https://doi.org/10.1172/jci.insight.85851.

29. Donermeyer, D.L., Beisel, K.W., Allen, P.M., and Smith, S.C. (1995). Myocarditis-inducing epitope of myosin binds constitutively and stably to I-Ak on antigen-presenting cells in the heart. J. Exp. Med. *182*, 1291–1300. https://doi.org/10.1084/jem.182.5.1291.

30. Pummerer, C.L., Luze, K., Grässl, G., Bachmaier, K., Offner, F., Burrell, S.K., Lenz, D.M., Zamborelli, T.J., Penninger, J.M., and Neu, N. (1996). Identification of cardiac myosin peptides capable of inducing autoimmune myocarditis in BALB/c mice. J. Clin. Invest. *97*, 2057–2062. https://doi.org/10.1172/JCI118642.

31. Massilamany, C., Upadhyaya, B., Gangaplara, A., Kuszynski, C., and Reddy, J. (2011). Detection of autoreactive CD4 T cells using major histocompatibility complex class II dextramers. BMC Immunol. *12*, 40. https://doi.org/10.1186/1471-2172-12-40.

32. Waldman, A.D., Fritz, J.M., and Lenardo, M.J. (2020). A guide to cancer immunotherapy: from T cell basic science to clinical practice. Nat. Rev. Immunol. *20*, 651–668. https://doi.org/10.1038/s41577-020-0306-5.

33. Massilamany, C., Gangaplara, A., Basavalingappa, R.H., Rajasekaran, R.A., Khalilzad-Sharghi, V., Han, Z., Othman, S., Steffen, D., and Reddy, J. (2016). Localization of CD8 T cell epitope within cardiac myosin heavy chain-alpha334-352 that induces autoimmune myocarditis in A/J mice. Int. J. Cardiol. *202*, 311–321. https://doi.org/10.1016/j.ijcard.2015.09.016.

34. Basavalingappa, R.H., Arumugam, R., Lasrado, N., Yalaka, B., Massilamany, C., Gangaplara, A., Riethoven, J.J., Xiang, S.H., Steffen, D., and Reddy, J. (2020). Viral myocarditis involves the generation of autoreactive T cells with multiple antigen specificities that localize in lymphoid and non-lymphoid organs in the mouse model of CVB3 infection. Mol. Immunol. *124*, 218–228. https://doi.org/10.1016/j.molimm.2020.06.017.

35. Michel, L., Helfrich, I., Hendgen-Cotta, U.B., Mincu, R.I., Korste, S., Mrotzek, S.M., Spomer, A., Odersky, A., Rischpler, C., Herrmann, K., et al. (2022). Targeting early stages of cardiotoxicity from anti-PD1 immune checkpoint inhibitor therapy. Eur. Heart J. *43*, 316–329. https://doi.org/10.1093/eurheartj/ehab430.

36. Rose, N.R., Wolfgram, L.J., Herskowitz, A., and Beisel, K.W. (1986). Post-infectious autoimmunity: two distinct phases of coxsackievirus B3-induced myocarditis. Ann. N. Y. Acad. Sci. *475*, 146–156. https://doi.org/10.1111/j.1749-6632.1986.tb20864.x.

37. Neu, N., Rose, N.R., Beisel, K.W., Herskowitz, A., Gurri-Glass, G., and Craig, S.W. (1987). Cardiac myosin induces myocarditis in genetically predisposed mice. J. Immunol. *139*, 3630–3636.

38. Cihák̀ová, D., Sharma, R.B., Fairweather, D., Afanasyeva, M., and Rose, N.R. (2004). Animal models for autoimmune myocarditis and autoimmune

thyroiditis. Methods Mol. Med. *102*, 175–193. https://doi.org/10.1385/1-59259-805-6:175.

39. Göser, S., Andrassy, M., Buss, S.J., Leuschner, F., Volz, C.H., Ottl, R., Zittrich, S., Blaudeck, N., Hardt, S.E., Pfitzer, G., et al. (2006). Cardiac troponin I but not cardiac troponin T induces severe autoimmune inflammation in the myocardium. Circulation *114*, 1693–1702. https://doi.org/10.1161/CIRCULATIONAHA.106.635664.
40. Ho, M., Post, C.M., Donahue, L.R., Lidov, H.G.W., Bronson, R.T., Goolsby, H., Watkins, S.C., Cox, G.A., and Brown, R.H., Jr. (2004). Disruption of muscle membrane and phenotype divergence in two novel mouse models of dysferlin deficiency. Hum. Mol. Genet. *13*, 1999–2010. https://doi.org/10.1093/hmg/ddh212.
41. Keithley, E.M., Canto, C., Zheng, Q.Y., Fischel-Ghodsian, N., and Johnson, K.R. (2004). Age-related hearing loss and the ahl locus in mice. Hear. Res. *188*, 21–28. https://doi.org/10.1016/S0378-5955(03)00365-4.
42. Hoag, W.G. (1963). Spontaneous cancer in mice. Ann. N. Y. Acad. Sci. *108*, 805–831. https://doi.org/10.1111/j.1749-6632.1963.tb13421.x.
43. Lucas, J.A., Menke, J., Rabacal, W.A., Schoen, F.J., Sharpe, A.H., and Kelley, V.R. (2008). Programmed death ligand 1 regulates a critical checkpoint for autoimmune myocarditis and pneumonitis in MRL mice. J. Immunol. *181*, 2513–2521. https://doi.org/10.4049/jimmunol.181.4.2513.
44. Adam, K., Iuga, A., Tocheva, A.S., and Mor, A. (2021). A novel mouse model for checkpoint inhibitor-induced adverse events. PLoS One *16*, e0246168. https://doi.org/10.1371/journal.pone.0246168.
45. Wang, J., Yoshida, T., Nakaki, F., Hiai, H., Okazaki, T., and Honjo, T. (2005). Establishment of NOD-Pdcd1-/- mice as an efficient animal model of type I diabetes. Proc. Natl. Acad. Sci. USA *102*, 11823–11828. https://doi.org/10.1073/pnas.0505497102.
46. Tivol, E.A., Borriello, F., Schweitzer, A.N., Lynch, W.P., Bluestone, J.A., and Sharpe, A.H. (1995). Loss of CTLA-4 leads to massive lymphoproliferation and fatal multiorgan tissue destruction, revealing a critical negative regulatory role of CTLA-4. Immunity *3*, 541–547. https://doi.org/10.1016/1074-7613(95)90125-6.
47. Klocke, K., Sakaguchi, S., Holmdahl, R., and Wing, K. (2016). Induction of autoimmune disease by deletion of CTLA-4 in mice in adulthood. Proc. Natl. Acad. Sci. USA *113*, E2383–E2392. https://doi.org/10.1073/pnas.1603892113.
48. Gangaplara, A., Massilamany, C., Brown, D.M., Delhon, G., Pattnaik, A.K., Chapman, N., Rose, N., Steffen, D., and Reddy, J. (2012). Coxsackievirus B3 infection leads to the generation of cardiac myosin heavy chain-alpha-reactive CD4 T cells in A/J mice. Clin. Immunol. *144*, 237–249. https://doi.org/10.1016/j.clim.2012.07.003.
49. Latif, N., Zhang, H., Archard, L.C., Yacoub, M.H., and Dunn, M.J. (1999). Characterization of anti-heart antibodies in mice after infection with coxsackie B3 virus. Clin. Immunol. *91*, 90–98. https://doi.org/10.1006/clim.1998.4679.
50. Wu, L., Diny, N.L., Ong, S., Barin, J.G., Hou, X., Rose, N.R., Talor, M.V., and Čihákova, D. (2016). Pathogenic IL-23 signaling is required to initiate GM-CSF-driven autoimmune myocarditis in mice. Eur. J. Immunol. *46*, 582–592. https://doi.org/10.1002/eji.201545924.
51. Nindl, V., Maier, R., Ratering, D., De Giuli, R., Züst, R., Thiel, V., Scandella, E., Di Padova, F., Kopf, M., Rudin, M., et al. (2012). Cooperation of Th1 and Th17 cells determines transition from autoimmune myocarditis to dilated cardiomyopathy. Eur. J. Immunol. *42*, 2311–2321. https://doi.org/10.1002/eji.201142209.
52. Nussinovitch, U., and Shoenfeld, Y. (2013). The clinical and diagnostic significance of anti-myosin autoantibodies in cardiac disease. Clin. Rev. Allergy Immunol. *44*, 98–108. https://doi.org/10.1007/s12016-010-8229-8.
53. Caforio, A.L.P., Mahon, N.J., Tona, F., and McKenna, W.J. (2002). Circulating cardiac autoantibodies in dilated cardiomyopathy and myocarditis: pathogenetic and clinical significance. Eur. J. Heart Fail. *4*, 411–417. https://doi.org/10.1016/s1388-9842(02)00010-7.
54. Grabie, N., Gotsman, I., DaCosta, R., Pang, H., Stavrakis, G., Butte, M.J., Keir, M.E., Freeman, G.J., Sharpe, A.H., and Lichtman, A.H. (2007). Endothelial programmed death-1 ligand 1 (PD-L1) regulates CD8+ T-cell mediated injury in the heart. Circulation *116*, 2062–2071. https://doi.org/10.1161/CIRCULATIONAHA.107.709360.
55. Bracamonte-Baran, W., Gilotra, N.A., Won, T., Rodriguez, K.M., Talor, M.V., Oh, B.C., Griffin, J., Wittstein, I., Sharma, K., Skinner, J., et al. (2021). Endothelial stromal PD-L1 (programmed death ligand 1) modulates CD8(+) T-cell infiltration after heart transplantation. Circ. Heart Fail. *14*, e007982. https://doi.org/10.1161/CIRCHEARTFAILURE.120.007982.
56. Berner, A.M., Sharma, A., Agarwal, S., Al-Sam, S., and Nathan, P. (2018). Fatal autoimmune myocarditis with anti-PD-L1 and tyrosine kinase inhibitor therapy for renal cell cancer. Eur. J. Cancer *101*, 287–290. https://doi.org/10.1016/j.ejca.2018.06.021.
57. Touat, M., Maisonobe, T., Knauss, S., Ben Hadj Salem, O., Hervier, B., Auré, K., Szwebel, T.A., Kramkimel, N., Lethrosne, C., Bruch, J.F., et al. (2018). Immune checkpoint inhibitor-related myositis and myocarditis in patients with cancer. Neurology *91*, e985-e994. https://doi.org/10.1212/WNL.0000000000006124.
58. Afanasyeva, M., Wang, Y., Kaya, Z., Stafford, E.A., Dohmen, K.M., Sadighi Akha, A.A., and Rose, N.R. (2001). Interleukin-12 receptor/STAT4 signaling is required for the development of autoimmune myocarditis in mice by an interferon-gamma-independent pathway. Circulation *104*, 3145–3151. https://doi.org/10.1161/hc5001.100629.
59. Frisancho-Kiss, S., Nyland, J.F., Davis, S.E., Frisancho, J.A., Barrett, M.A., Rose, N.R., and Fairweather, D. (2006). Sex differences in coxsackievirus B3-induced myocarditis: IL-12Rbeta1 signaling and IFN-gamma increase inflammation in males independent from STAT4. Brain Res. *1126*, 139–147. https://doi.org/10.1016/j.brainres.2006.08.003.
60. Eriksson, U., Kurrer, M.O., Sebald, W., Brombacher, F., and Kopf, M. (2001). Dual role of the IL-12/IFN-gamma axis in the development of autoimmune myocarditis: induction by IL-12 and protection by IFN-gamma. J. Immunol. *167*, 5464–5469. https://doi.org/10.4049/jimmunol.167.9.5464.
61. Fairweather, D., Frisancho-Kiss, S., Yusung, S.A., Barrett, M.A., Davis, S.E., Steele, R.A., Gatewood, S.J.L., and Rose, N.R. (2005). IL-12 protects against coxsackievirus B3-induced myocarditis by increasing IFN-gamma and macrophage and neutrophil populations in the heart. J. Immunol. *174*, 261–269. https://doi.org/10.4049/jimmunol.174.1.261.
62. Grabie, N., Delfs, M.W., Westrich, J.R., Love, V.A., Stavrakis, G., Ahmad, F., Seidman, C.E., Seidman, J.G., and Lichtman, A.H. (2003). IL-12 is required for differentiation of pathogenic CD8+ T cell effectors that cause myocarditis. J. Clin. Invest. *111*, 671–680. https://doi.org/10.1172/JCI16867.
63. Garris, C.S., Arlauckas, S.P., Kohler, R.H., Trefny, M.P., Garren, S., Piot, C., Engblom, C., Pfirschke, C., Siwicki, M., Gungabeesoon, J., et al. (2018). Successful anti-PD-1 cancer immunotherapy requires T cell-dendritic cell crosstalk involving the cytokines IFN-gamma and IL-12. Immunity *49*, 1148, 1161.e7. https://doi.org/10.1016/j.immuni.2018.09.024.
64. Algazi, A.P., Twitty, C.G., Tsai, K.K., Le, M., Pierce, R., Browning, E., Hermiz, R., Canton, D.A., Bannavong, D., Oglesby, A., et al. (2020). Phase II trial of IL-12 plasmid transfection and PD-1 blockade in immunologically quiescent melanoma. Clin. Cancer Res. *26*, 2827–2837. https://doi.org/10.1158/1078-0432.CCR-19-2217.
65. Lv, H., Havari, E., Pinto, S., Gottumukkala, R.V.S.R.K., Cornivelli, L., Raddassi, K., Matsui, T., Rosenzweig, A., Bronson, R.T., Smith, R., et al. (2011). Impaired thymic tolerance to alpha-myosin directs autoimmunity to the heart in mice and humans. J. Clin. Invest. *121*, 1561–1573. https://doi.org/10.1172/JCI44583.
66. Montacchiesi, G., and Pace, L. (2022). Epigenetics and CD8(+) T cell memory. Immunol. Rev. *305*, 77–89. https://doi.org/10.1111/imr.13057.
67. Baaten, B.J.G., Tinoco, R., Chen, A.T., and Bradley, L.M. (2012). Regulation of antigen-experienced T cells: lessons from the quintessential

memory marker CD44. Front. Immunol. *3*, 23. https://doi.org/10.3389/fimmu.2012.00023.

68. Ahn, E., Araki, K., Hashimoto, M., Li, W., Riley, J.L., Cheung, J., Sharpe, A.H., Freeman, G.J., Irving, B.A., and Ahmed, R. (2018). Role of PD-1 during effector CD8 T cell differentiation. Proc. Natl. Acad. Sci. USA *115*, 4749–4754. https://doi.org/10.1073/pnas.1718217115.

69. Gil-Cruz, C., Perez-Shibayama, C., De Martin, A., Ronchi, F., van der Borght, K., Niederer, R., Onder, L., Lütge, M., Novkovic, M., Nindl, V., et al. (2019). Microbiota-derived peptide mimics drive lethal inflammatory cardiomyopathy. Science *366*, 881–886. https://doi.org/10.1126/science.aav3487.

70. Massilamany, C., Gangaplara, A., Steffen, D., and Reddy, J. (2011). Identification of novel mimicry epitopes for cardiac myosin heavy chain-alpha that induce autoimmune myocarditis in A/J mice. Cell. Immunol. *271*, 438–449. https://doi.org/10.1016/j.cellimm.2011.08.013.

71. Yoshikawa, T., Baba, A., and Nagatomo, Y. (2009). Autoimmune mechanisms underlying dilated cardiomyopathy. Circ. J. *73*, 602–607. https://doi.org/10.1253/circj.cj-08-1151.

72. Kallwellis-Opara, A., Dörner, A., Poller, W.C., Noutsias, M., Kühl, U., Schultheiss, H.P., and Pauschinger, M. (2007). Autoimmunological features in inflammatory cardiomyopathy. Clin. Res. Cardiol. *96*, 469–480. https://doi.org/10.1007/s00392-007-0524-x.

73. Xie, X., Wang, L., Li, Y., Xu, Y., Wu, J., Lin, X., Lin, W., Mai, Q., Chen, Z., Zhang, J., et al. (2022). Multi-organ immune-related adverse event is a risk factor of immune checkpoint inhibitor-associated myocarditis in cancer patients: a multi-center study. Front. Immunol. *13*, 879900. https://doi.org/10.3389/fimmu.2022.879900.

74. Wetsel, R.A., Fleischer, D.T., and Haviland, D.L. (1990). Deficiency of the murine fifth complement component (C5). A 2-base pair gene deletion in a 5'-exon. J. Biol. Chem. *265*, 2435–2440.

75. Jagannath, C., Hoffmann, H., Sepulveda, E., Actor, J.K., Wetsel, R.A., and Hunter, R.L. (2000). Hypersusceptibility of A/J mice to tuberculosis is in part due to a deficiency of the fifth complement component (C5). Scand. J. Immunol. *52*, 369–379. https://doi.org/10.1046/j.1365-3083.2000.00770.x.

76. Gervais, F., Stevenson, M., and Skamene, E. (1984). Genetic control of resistance to Listeria monocytogenes: regulation of leukocyte inflammatory responses by the Hc locus. J. Immunol. *132*, 2078–2083.

77. Meder, B., Rühle, F., Weis, T., Homuth, G., Keller, A., Franke, J., Peil, B., Lorenzo Bermejo, J., Frese, K., Huge, A., et al. (2014). A genome-wide association study identifies 6p21 as novel risk locus for dilated cardiomyopathy. Eur. Heart J. *35*, 1069–1077. https://doi.org/10.1093/eurheartj/eht251.

78. Zamami, Y., Niimura, T., Okada, N., Koyama, T., Fukushima, K., Izawa-Ishizawa, Y., and Ishizawa, K. (2019). Factors associated with immune checkpoint inhibitor-related myocarditis. JAMA Oncol. *5*, 1635–1637. https://doi.org/10.1001/jamaoncol.2019.3113.

79. Root-Bernstein, R., and Fairweather, D. (2015). Unresolved issues in theories of autoimmune disease using myocarditis as a framework. J. Theor. Biol. *375*, 101–123. https://doi.org/10.1016/j.jtbi.2014.11.022.

80. Huang, X., Venet, F., Wang, Y.L., Lepape, A., Yuan, Z., Chen, Y., Swan, R., Kherouf, H., Monneret, G., Chung, C.S., and Ayala, A. (2009). PD-1 expression by macrophages plays a pathologic role in altering microbial clearance and the innate inflammatory response to sepsis. Proc. Natl. Acad. Sci. USA *106*, 6303–6308. https://doi.org/10.1073/pnas.0809422106.

81. Yao, S., Wang, S., Zhu, Y., Luo, L., Zhu, G., Flies, S., Xu, H., Ruff, W., Broadwater, M., Choi, I.H., et al. (2009). PD-1 on dendritic cells impedes innate immunity against bacterial infection. Blood *113*, 5811–5818. https://doi.org/10.1182/blood-2009-02-203141.

82. Mallett, G., Laurence, A., and Amarnath, S. (2019). Programmed cell death-1 receptor (PD-1)-Mediated regulation of innate lymphoid cells. Int. J. Mol. Sci. *20*, E2836. https://doi.org/10.3390/ijms20112836.

STAR★METHODS

KEY RESOURCES TABLE

REAGENT or RESOURCE	SOURCE	IDENTIFIER
Antibodies		
Anti-mouse PD-1 (clone RMP1-14)	Bio X Cell	Cat# BE0146; RRID: AB_10949053
Rat IgG2a isotype control (clone 2A3)	Bio X Cell	Cat# BE0089; RRID: AB_1107769
Anti-mouse CTLA-4 (clone UC-10-4F10-11)	Bio X Cell	Cat# BE0032; RRID: AB_1107598
Purified anti-CD16/CD32 (clone 93)	Thermo Fisher	Cat# 14-0161-86; RRID: AB_467133
BUV563 anti-mouse CD45 (clone 30-F11)	BD Biosciences	Cat# 612924; RRID: AB_2870209
APC anti-mouse NKp46 (clone 29A1.4)	BioLegend	Cat# 137607; RRID: AB_10612749
FITC anti-mouse CD11b (clone M1/70)	BioLegend	Cat# 101205; RRID: AB_312788
BV785 anti-mouse Ly6G (clone 1A8)	BioLegend	Cat# 127645; RRID: AB_2566317
PE-Cy7 anti-mouse F4/80 (clone BM8)	BioLegend	Cat# 123113; RRID: AB_893490
BV711 anti-mouse CD64 (clone X54-5/7.1)	BioLegend	Cat# 139311; RRID: AB_2563846
Alexa Fluor 700 anti-mouse Ly6C (clone HK1.4)	BioLegend	Cat# 128023; RRID: AB_10640119
BUV395 anti-mouse CD19 (clone 1D3)	BD Biosciences	Cat# 565965; RRID: AB_2739418
PE-Dazzle 594 anti-mouse CD3 (clone 17A2)	BioLegend	Cat# 100245; RRID: AB_2565882
BV421 anti-mouse TCR$\gamma\delta$ (clone GL3)	BioLegend	Cat# 118119; RRID: AB_10896753
BV605 anti-mouse CD4 (clone GK1.5)	BioLegend	Cat# 100451; RRID: AB_2564591
BUV805 anti-mouse CD8 (clone 53-6.7)	BD Biosciences	Cat# 612898; RRID: AB_2870186
BV421 anti-mouse CD62L (clone MEL-14)	BioLegend	Cat# 104435; RRID: AB_10900082
PE-Cy7 anti-mouse CD44 (clone IM7)	BioLegend	Cat# 103029; RRID: AB_830786
BUV395 anti-mouse CD69 (clone H1.2F3)	BD Biosciences	Cat# 740220; RRID: AB_2739968
BV711 anti-mouse PD-1 (clone 29F.1A12)	BioLegend	Cat# 135231; RRID: AB_2566158
BV605 anti-mouse TIM-3 (clone RMT3-23)	BioLegend	Cat# 119721; RRID: AB_2616907
CD4 (L3T4) MicroBeads, Mouse	Miltenyi	Cat# 130-117-043
Chemicals, peptides, and recombinant proteins		
Freund's Adjuvant, Complete	MilliporeSigma	Cat# F5881
Recombinant Murine IL-12p70	PeproTech	Cat# 210-12
Recombinant Mouse IL-23	Sino Biological	Cat# CT028-M08H
Recombinant Mouse IL-1beta	Sino Biological	Cat# 50101-MNAE
Collagenase, Type 2	Worthington	Cat# LS004177
Deoxyribonuclease I	Worthington	Cat# LS002139
Hyaluronidase	MilliporeSigma	Cat# H3506
Normal Rat Serum	Thermo Fisher	Cat# 31888; RRID: AB_2532178
RNeasy Plus Micro Kit	Qiagen	Cat# 74034
iScript Reverse Transcription Supermix	Bio-Rad	Cat# 7108841
PowerUP SYBR Green Master Mix	Thermo Fisher	Cat# A25742
Critical commercial assays		
LIVE/DEAD Fixable Aqua Dead Cell Stain Kit	Thermo Fisher	Cat# L34966
Mouse Cardiac Troponin-I ELISA	Life Diagnostics	Cat# CTNI-1-US
DeadEnd Fluorometric TUNEL System	Promega	Cat# G3250
Experimental models: Organisms/strains		
Male A/J mouse	Jackson Laboratory	Cat# 000646; RRID:IMSR_JAX:000646
Oligonucleotides		
Primers for real-time RT-PCR, see Table S2	Integrated DNA Technologies	N/A

(*Continued on next page*)

Continued

REAGENT or RESOURCE	SOURCE	IDENTIFIER
Software and algorithms		
FlowJo	BD	RRID: SCR_008520
Prism	GraphPad	RRID: SCR_002798

RESOURCE AVAILABILITY

Lead contact

Further information and requests for resources and reagents should be directed to and will be fulfilled by the lead contact, Daniela Čiháková (cihakova@jhmi.edu).

Materials availability

This study did not generate new unique reagents.

Data and code availability

All data reported in this paper will be shared by the lead contact upon request.
This paper does not report original code.
Any additional information required to reanalyze the data reported in this paper is available from the lead contact upon request.

EXPERIMENTAL MODEL AND SUBJECT DETAILS

Mice

Wild-type male A/J mice (strain #000646) were purchased from the Jackson Laboratory. Mice were housed in specific pathogen-free animal facilities at the Johns Hopkins University School of Medicine. Experiments were conducted with 8- to 12-week-old age-matched male mice. Thirty-six mice were injected with anti-PD-1 mAb (150 μg/mouse, clone RMP1-14, Bio X Cell) intraperitoneally every three days for 21 days. As a control, 25 mice were injected with rat IgG2a isotype mAb (Bio X Cell). Mice were supplemented with CFA (MilliporeSigma), anti-CTLA-4 mAb (clone UC-10-4F10-11, Bio X Cell), or recombinant murine IL-12p70 (PeproTech) when indicated. CFA was emulsified by mixing with the same volume of PBS and subcutaneously injected into the flank of mice (100 μL/mouse) on days 0 and 7. Anti-CTLA-4 mAb (150 μg/mouse) or IL-12p70 (300 ng/mouse) was intraperitoneally injected every three days. In senescence or sex difference experiments, 44-week-old male mice or 8- to 12-week-old female mice were used. All methods and protocols were approved by the Animal Care and Use Committee of the Johns Hopkins University.

METHOD DETAILS

Histology study

All harvested tissues were fixed, paraffin-embedded, cut as 4-μm-thick sections, and stained with H&E. Myocarditis severity was assessed by microscopic assessment and shown as the percentage of inflamed area in the heart section. Inflammation in other organs was assessed as increased cellularity in parenchymal space of the lung, lamina propria in the colon, or quadriceps in the right hind limb compared to naïve mouse organs. Pancreatitis was assessed in the entire tissue section, not limited to islets. Grading was performed by two independent blinded investigators. Images were acquired on a BX43 microscope (Olympus) with a DS-Fi3 camera (Nikon) using NIS-Elements D Software (Nikon).

Electrocardiography

Mice were terminally anesthetized by intraperitoneal injection with Avertin (0.4 mg/g). Electrode on right lower limb was connected to ground. Other three limbs' electrodes were sequentially changed to obtain bipolar leads following standard human EKG pattern: Lead I (DI) trace - positive electrode on left upper limb and negative electrode on right upper limb; Lead II (DII) trace - positive electrode on right upper limb and negative electrode on left lower limb; Lead III (DIII) trace - positive electrode on left upper limb and negative lead on left lower limb, creating standard Einthoven's triangle. We used a bipolar polygrapher (DigiMed) running DMSI-400 software.

Single cell isolation

Hearts were minced using a razor blade and then incubated with 5 mL of tissue digestion enzyme solution for 30 minutes at 37°C with agitation. The digestion enzyme solution was prepared with 600 U/ml Collagenase (Worthington), 50 U/ml DNase I (Worthington), and 50 U/ml Hyaluronidase (MilliporeSigma). After incubation with digestion enzymes, tissues were dissociated using gentleMACS Dissociator (Miltenyi). Cells were washed and filtered through 40 μm cell strainers (Falcon). Spleen and lymph node cells were mechanically dissociated from tissues using frosted-end glass slides. PBMCs were isolated using density gradient centrifugation.

Flow cytometry

Heart cells were stained with viability marker Live/Dead Fixable Aqua (Thermo Fisher) and then Fc-blocked with anti-CD16/32 mAb (Thermo Fisher) and normal rat serum (Thermo Fisher). Next, cells were surface-stained with fluorochrome-conjugated antibodies against CD45, NKp46, CD11b, Ly6G, F4/80, CD64, Ly6C, CD19, CD3, TCR$\gamma\delta$, CD4, CD8, CD62L, CD44, CD69, PD-1, and TIM-3 (BioLegend or BD Biosciences). For tetramer staining, cells were stained with $Myhc_{338\text{-}348}$-H-$2D^d$ and $Myhc_{334\text{-}352}$-I-A^k tetramers or $HIV_{P18\text{-}I10}$-H-$2D^d$ and human $CLIP_{87\text{-}101}$-I-A^k tetramers as a control before viability marker staining. Dr. Jay Reddy (University of Nebraska-Lincoln) and NIH Tetramer Core Facility kindly provided tetramers. Sample acquisition was performed on a BD LSR II or LSRFortessa flow cytometer (BD) running FACSDiva (BD). Results were analyzed using FlowJo software (BD). For FACS sorting, BD FACSAria IIu Cell Sorter was used.

ELISA

For determining cTnI levels in mouse serum, we used ELISA kit according to the manufacturer's instruction (Life Diagnostics). For anti-cardiac myosin and cTnI IgG ELISA, microplates were coated with 0.5 μg/mL cardiac myosin peptide (DSAFDVLSFTAEE KAGVYK) or cTnI peptide (VDKVDEERYDVEAKVTKN) overnight at 4°C, washed, and incubated with mouse serum for 2 hours at room temperature. Microplates were washed, incubated with secondary anti-mouse IgG antibody (Abcam), and developed with alkaline phosphatase (Bio-Rad). Optical density was read at 405 nm (Molecular Devices).

TUNEL assay

To detect apoptotic cells in the heart, we stained tissue sections with TUNEL according to the manufacturer's instruction (Promega). Mouse heart slides were deparaffinized, rehydrated, fixed, and permeablized. After equilibration, slides were probed with fluorescein-12-dUTP using terminal deoxynucleotidyl transferase (TdT). The slides were counterstained with DAPI to visualize all nuclei. Images were acquired using LSM 700 microscope (Zeiss).

Real-time RT-PCR

Total RNA from FACS-sorted cells was extracted using RNeasy Plus Micro Kit (Qiagen). Single-stranded cDNA was synthesized with iScript Reverse Transcription Supermix (Bio-Rad). Target genes were amplified using PowerUP SYBR Green PCR Master Mix (Applied Biosystems), and real-time cycle thresholds were detected via MyiQ2 thermal cycler (Bio-Rad). Data were analyzed by the $2^{-\Delta\Delta Ct}$ method and were normalized to *HPRT* expression and then to biological controls.

Adoptive transfer of T cells

$CD4^+$ T cells primed with cardiac myosin peptide were adoptively transferred into recipient mice to induce myocarditis, as previously published.[50] Donor mice were immunized with $Myhc_{334\text{-}352}$ peptide on days 0 and 7. Spleen cells were isolated on day 14 and then *in vitro* stimulated with 50 μg/mL $Myhc_{334\text{-}352}$ peptide, 20 ng/mL recombinant IL-23, 10 ng/mL recombinant IL-1β, and 40 mM NaCl. As a control, spleens cells from naïve mice were stimulated in the same manner. After four days of *in vitro* culture, $CD4^+$ T cells were sorted using magnetic beads-labeled Ab (Miltenyi) and intravenously injected into mice irradiated with 500 cGy γ-radiation (1×10^6 cells/recipient). All recipients were treated with 150 μg of anti-PD-1 mAb every three days, and their hearts were harvested 18 days after T cell transfer to evaluate myocarditis development. Where indicated, as donor cells, $Myhc_{334\text{-}352}$ tetramer-positive $CD4^+$ T cells were FACS-sorted from naïve mouse spleens and *in vitro* expanded with anti-CD3 and CD28 antibodies (2.5 μg/mL each). Tetramer-negative $CD4^+$ T cells were also sorted and *in vitro* stimulated to serve as a control. Those T cells were adoptively transferred to irradiated recipients that were treated with anti-PD-1 mAb after transfer.

QUANTIFICATION AND STATISTICAL ANALYSIS

Statistics

GraphPad Prism 9 software was used for statistical analysis. Data were analyzed using Student's *t*-test or one-way ANOVA followed by Tukey's multiple comparison test. Statistically significant comparisons were represented by asterisks: *, $p < 0.05$; **, $p < 0.005$; ***, $p < 0.0005$; ****, $p < 0.0001$.